
FINAL

Combustion 2000
Phase II

DE-AC22-95PC95144--27

Quarterly Progress Report

January 1 - March 31, 2000

Prepared for

**Federal Energy Technology Center
Pittsburgh, Pennsylvania**

**United Technologies Research Center
411 Silver Lane, East Hartford, Connecticut 06108**

“This report was prepared as an account of work sponsored by an agency of the United States government. Neither the United States Government nor any agency thereof, nor any of their employees, makes any warranty, express or implied, or assumes any legal liability or responsibility for the accuracy, completeness, or usefulness of any information, apparatus, product, or process disclosed, or represents that its use would not infringe privately owned rights. Reference herein to any specific commercial product, process, or service by trade name, trademark, manufacturer, or otherwise does not necessarily constitute or imply its endorsement, recommendation, or favoring by the United States Government or any agency thereof. The views and opinions of authors expressed herein do not necessarily state or reflect those of the United States Government or any agency thereof.”

FINAL

Combustion 2000
Phase II

DE-AC22-95PC95144

Quarterly Progress Report

January 1 - March 31, 2000

Prepared for

**Federal Energy Technology Center
Pittsburgh, Pennsylvania**

**United Technologies Research Center
411 Silver Lane, East Hartford, Connecticut 06108**

Table of Contents

| | |
|---|-----|
| List of Exhibits | iii |
| List of Tables | v |
| Abstract..... | vii |
| Executive Summary..... | ix |
| Introduction | 1 |
| Task 2.2.4 – Pilot-Scale Testing..... | 2 |
| Description of Pilot-Scale SFS..... | 2 |
| Pilot-Scale SFS Activities This Quarter | 9 |
| Testing of the CAH Tube Bank | 25 |
| Testing of the RAH Panel..... | 32 |
| Task 2.2.5 – Laboratory- and Bench-Scale Activities | 46 |
| Task 6.4 HIPPS Repowering | 52 |
| 6.4.1 Performance | 52 |
| 6.4.2 Economic Comparison..... | 53 |
| 6.4.3 Repowering of AFB Plant | 56 |
| Reference | 58 |

List of Exhibits

| | | |
|--------------|--|----|
| Exhibit 2-1 | Combustion 2000 Slagging Furnace and Support Systems | 2 |
| Exhibit 2-2 | Illustration of the Tubes in the CAH Tube Bank | 8 |
| Exhibit 2-3 | Coal Feed Rate Versus Run Time for the December Test, SFS-RH11-0799..... | 10 |
| Exhibit 2-4 | Furnace and Slag Screen Temperatures Versus Run Time for the December Test, SFS-RH11-0799 | 14 |
| Exhibit 2-5 | Slagging Furnace Firing Rate Versus Run Time for the December Test, SFS-RH11-0799..... | 15 |
| Exhibit 2-6 | Photograph of Furnace Interior Following the December Test, SFS-RH11-0799..... | 16 |
| Exhibit 2-7 | Photograph of the Slag Screen Inlet Following the December Test, SFS-RH11-0799..... | 18 |
| Exhibit 2-8 | Process Air Preheater Temperatures Versus Run Time for the December Test, SFS-RH11-0799..... | 20 |
| Exhibit 2-9 | Respirable Mass Emissions Data for the December Test | 23 |
| Exhibit 2-10 | CAH Tube Surface and Flue Gas Temperatures Versus Run Time for the December Test, SFS-RH11-0799 | 26 |
| Exhibit 2-11 | CAH Process Air Temperatures Versus Run Time for the December Test, SFS-RH11-0799..... | 26 |
| Exhibit 2-12 | CAH Process Air, RAH Process Air, Quench Gas, and Flue Gas Flow Rates Versus Run Time for the December Test, SFS-RH11-0799 | 27 |
| Exhibit 2-13 | Thermocouple Locations in the CAH Tube Bank | 27 |
| Exhibit 2-14 | CAH Heat Recovery Versus Run Time for the December Test, SFS-RH11-0799..... | 30 |
| Exhibit 2-15 | Photograph of Ash Deposits on the CAH tubes Following the December Test Firing Illinois No. 6 Bituminous Coal | 31 |
| Exhibit 2-16 | Illustration of Cracks Found in the New and Used Ceramic Tiles/Bricks Installed in the RAH Panel Prior to the December Test, SFS-RH11-0799..... | 33 |
| Exhibit 2-17 | Photograph of the Ceramic Tiles Installed on the RAH Panel Prior to the December Test | 34 |
| Exhibit 2-18 | Photograph of the RAH Panel Inside of the Slagging Furnace Following the December Test | 35 |
| Exhibit 2-19 | Illustration of Cracks Found in the Ceramic Tiles/Bricks of the RAH Panel Following the December Test..... | 36 |
| Exhibit 2-20 | Photograph of the Large Kyocera Tile Following the December Test..... | 37 |

| | | |
|---------------|--|----|
| Exhibit 2-21 | Photograph of the RAH Small Lower Tile Following the December Test | 38 |
| Exhibit 2-22 | RAH Ceramic Tile Temperatures Versus Run Time for the December Test, SFS-RH11-0799..... | 40 |
| Exhibit 2-23 | RAH Tube Surface Temperatures Versus Run Time for the December Test, SFS-RH11-0799..... | 40 |
| Exhibit 2-24 | RAH Process Air Temperatures Versus Run Time for the December Test, SFS-RH11-0799..... | 41 |
| Exhibit 2-25 | Thermocouple Locations in the RAH Panel..... | 41 |
| Exhibit 2-26 | RAH Heat Recovery Versus Run Time for the December Test, SFS-RH11-0799..... | 43 |
| Exhibit 2-27 | RAH Heat Recovery for Bituminous Coal-Fired Tests Completed in 1998 and 1999 | 44 |
| Exhibit 2-28 | Cumulative Corrosion of Alloy MA-754 at 2100°F (1150°C) and 1832°F (1000°C)..... | 47 |
| Exhibit 2-29 | SEM Micrograph of Alloy MA-754 Showing Oxide Layer | 48 |
| Exhibit 2-30 | X-Ray Maps of Alloy MA-754 Showing Oxide Layer..... | 49 |
| Exhibit 2-31 | X-Ray Maps of Alloy MA-754 Showing Crystallites | 50 |
| Exhibit 2-32 | SEM Micrograph of Alloy Ma-754 Showing Crystallites in the Slag Layer | 50 |
| Exhibit 6.4.1 | Schematic of HIPPS/SOFC Repowering..... | 52 |
| Exhibit 6.4.2 | Projected Fuel Cost Ratio | 55 |
| Exhibit 6.4.3 | Relative Cost of Electricity..... | 55 |
| Exhibit 6.4.4 | Relative COE with CO ₂ Removal..... | 56 |
| Exhibit 6.4.5 | Schematic of Nominal 160 MW TVA AFB..... | 57 |

List of Tables

| | | |
|-------------|---|----|
| Table 2-1 | Refractory Properties | 5 |
| Table 2-2 | Results of Coal and Coal Ash Analysis for Coal-Fired Slagging Furnace Tests..... | 12 |
| Table 2-3 | Analysis of Lignite and Lignite Ash Slagging Furnace Tests..... | 13 |
| Table 2-4 | Slag Screen Flue Gas Composition for the Illinois No. 6 Coal-Fired SFS Test..... | 25 |
| Table 2-5 | Description of CAH Thermocouple Locations..... | 29 |
| Table 2-6 | Description of RAH Panel Thermocouple Locations..... | 39 |
| Table 2-7 | Summary of Operating Hours for the SFS, CAH Tube Bank, and RAH Panel Through February 2000 | 45 |
| Table 2-8 | Elemental Concentrations of the Oxidation Products, wt%..... | 51 |
| Table 6.4.1 | HIPPS/SOFC Performance | 53 |

Abstract

This report presents work carried out under contract DE-AC22-95PC95144 "Combustion 2000 - Phase II." The goals of the program are to develop a coal-fired high performance power generation system (HIPPS) that is capable of:

- ◇ thermal efficiency (HHV) $\geq 47\%$
- ◇ NO_x, SO_x, and particulates $\leq 10\%$ NSPS
(New Source Performance Standard)
- ◇ coal providing $\geq 65\%$ of heat input
- ◇ all solid wastes benign
- ◇ cost of electricity $\leq 90\%$ of present plants

Phase I, which began in 1992, focused on the analysis of various configurations of indirectly fired cycles and on technical assessments of alternative plant subsystems and components, including performance requirements, developmental status, design options, complexity and reliability, and capital and operating costs. Phase I also included preliminary R&D and the preparation of designs for HIPPS commercial plants approximately 300 MWe in size.

Phase II, had as its initial objective the development of a complete design base for the construction and operation of a HIPPS prototype plant to be constructed in Phase III. As part of a descoping initiative, the Phase III program has been eliminated and work related to the commercial plant design has been ended. The rescoped program retained a program of engineering research and development focusing on high temperature heat exchangers, e.g. HITAF development (Task 2); a rescoped Task 6 that is pertinent to Vision 21 objectives and focuses on advanced cycle analysis and optimization, integration of gas turbines into complex cycles, and repowering designs; and preparation of the Phase II Technical Report (Task 8). This rescoped program deleted all subsystem testing (Tasks 3, 4, and 5) and the development of a site-specific engineering design and test plan for the HIPPS prototype plant (Task 7).

Work reported herein is from:

- ◇ Task 2.2.4 Pilot Scale Testing
- ◇ Task 2.2.5.2 Laboratory and Bench Scale Activities
- ◇ Task 6.4 HIPPS Repowering

Executive Summary

This report represents work carried out under contract DE-AC22-95PC95144 "Combustion 2000: Phase II." The goals of the program are to develop a coal-fired high performance power generation system (HIPPS) that is capable of:

- ◇ $\geq 47\%$ thermal efficiency (HHV)
- ◇ NO_x , SO_x , and particulates $\leq 10\%$ NSPS
- ◇ coal providing $\geq 65\%$ of heat input
- ◇ all solid wastes benign
- ◇ cost of electricity $\leq 90\%$ of present plant

Work reported in this report is from Task 2.2 HITAF Air Heaters and Task 6.4 HIPPS Repowering.

Data and observations from coal-fired tests completed in December 1999 are documented in this report and compared with previous data where appropriate. The December 1999 data, results, and observations are included in this report because they were not available for inclusion in the quarterly technical progress report for October through December 1999. In addition, the performance of the radiant air heater (RAH) panel was evaluated during one SFS test period this past quarter (March 19–31). However, results from the SFS test completed in March are incomplete at this time and will be summarized in the quarterly technical progress report for April through June 2000. This report also includes data from laboratory testing of the corrosion resistance of the MA 754 alloy, including a discussion of a possible temperature window over which the products of coal combustion are much less corrosive toward structural materials.

Summary of Operating Hours for the SFS, CAH Tube Bank, and RAH Panel Through February 2000

| | Natural Gas Firing, hr | Coal/Lignite Firing, hr | Total Operation, hr |
|-------------------------|------------------------|-------------------------|---------------------|
| Slagging Furnace System | 1737 | 1182 | 2919 |
| CAH Tube Bank | 1422 | 1149 | 2571 |
| RAH Panel | 1238 | 1102 | 2340 |

The results of a repowering study using HIPPS technology combined with a solid oxide fuel cell are also presented here. The performance and economic analysis show this configuration to be particularly flexible and to offer high overall efficiencies.

Introduction

The High Performance Power Systems (HIPPS) electric power generation plant integrates a combustion gas turbine and heat recovery steam generator (HRSG) combined cycle arrangement with an advanced coal-fired boiler. The unique feature of the HIPPS plant is the partial heating of gas turbine (GT) compressor outlet air using energy released by firing coal in the high temperature advanced furnace (HITAF). The compressed air is additionally heated prior to entering the GT expander section by burning natural gas. Thermal energy in the gas turbine exhaust and in the HITAF flue gas are used in a steam cycle to maximize electric power production. The HIPPS plant arrangement is thus a combination of existing technologies (gas turbine, heat recovery boilers, conventional steam cycle) and new technologies (the HITAF design including the air heaters, and especially the heater located in the radiant section).

The HITAF provides heat to the compressor outlet air using two air heaters, a convective air heater (CAH), and a radiant air heater (RAH). The HITAF is a slagging furnace which contains the radiant air heater, as well as waterwalls and steam drum for the high pressure (HP) steam system. Hot flue gas leaving the HITAF furnace passes over the CAH prior to entering a heat recovery steam generator (HRSG). Hot exhaust gas from the gas turbine is ducted to another HRSG in a typical combined cycle arrangement. The HITAF, gas turbine and HRSGs are configured to achieve the required high efficiency of the HIPPS plant.

The key to the success of the concept is the development of integrated combustor/air heater that will fire a wide range of US coals with minimal natural gas and with the reliability of current coal-fired plants. The compatibility of the slagging combustor with the high temperature radiant air heater is the critical challenge.

Task 2.2.4 – Pilot-Scale Testing

Pilot-scale activities this past quarter were performed under Task 2.2.4.3, HITAF Testing. They involved SFS maintenance, modifications and repairs, and completion of a 200-hr coal-fired SFS test in March. Instrumentation work this past quarter focused on routine maintenance and calibration of SFS components. Other activities were limited to miscellaneous maintenance items in support of overall SFS operation, selection and procurement of a subbituminous coal for the March test, reconstruction of the slag screen prior to the March test, and completion of a 200-hr coal-fired SFS test on March 31, 2000. Funding for these activities was provided through the subcontract to UTRC for Combustion 2000 work.

Description of Pilot-Scale SFS

Exhibit 2-1 (exhibits follow text) is a simplified illustration of the overall slagging furnace system. There have been no changes to the exhibit in the past quarter.

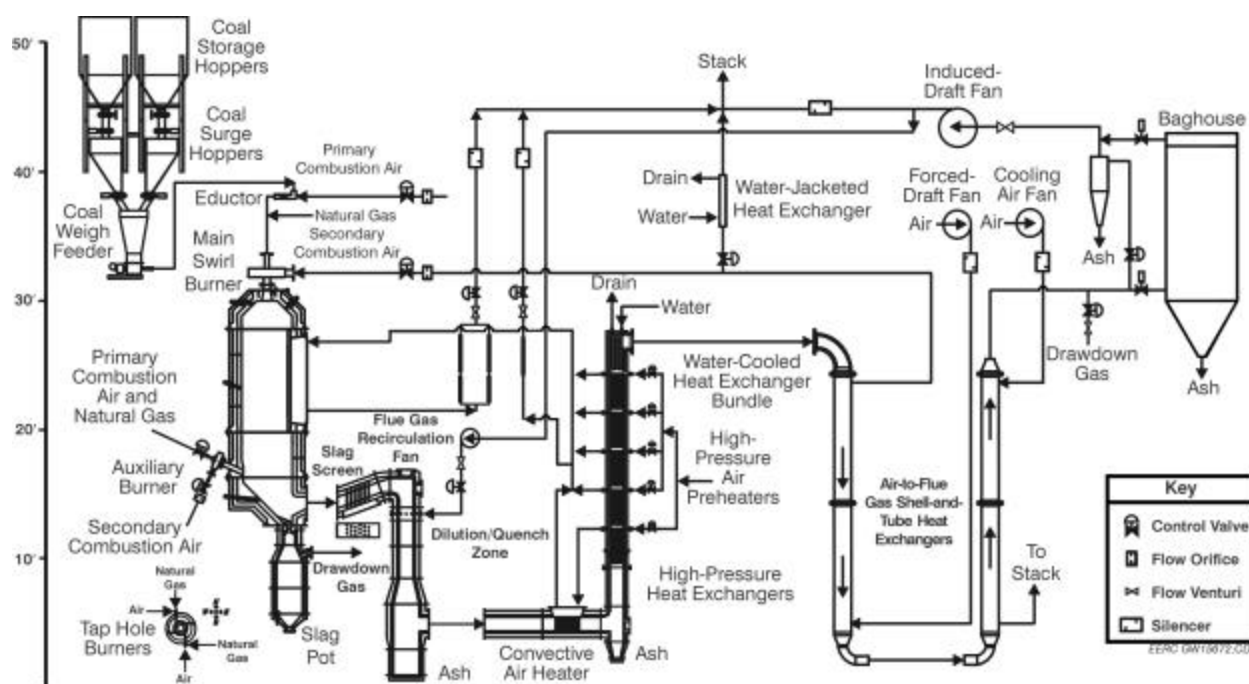


Exhibit 2-1
Combustion 2000 Slagging Furnace and Support Systems

Slagging Furnace

The pilot-scale slagging furnace design is intended to be as fuel-flexible as possible, with maximum furnace exit temperatures of 2700° to 2900°F (1483° to 1593°C) to maintain the desired heat transfer to the RAH panel and slag flow. The furnace has a nominal firing rate of 2.5 MMBtu/hr (2.6×10^6 kJ/hr) and a range of 2.0 to 3.0 MMBtu/hr (2.1 to 3.2×10^6 kJ/hr) using a single burner. The design is based on Illinois No. 6 bituminous coal (11,100 Btu/lb, or 25,800 kJ/kg) and a nominal furnace residence time of 3.5 s. Flue gas flow rates range from roughly 425 to 645 scfm (12.0 to 18.6 m³/min), with a nominal value of 530 scfm (15 m³/min), based on 20%

excess air. Firing a subbituminous coal or lignite increases the flue gas volume, decreasing residence time to roughly 2.6 s. However, the high volatility of the low-rank fuels results in high combustion efficiency (>99%). The EERC oriented the furnace vertically (downfired) and based the burner design on that of a swirl burner used on two smaller EERC pilot-scale pulverized coal (pc)-fired units (600,000 Btu/hr [633,000 kJ/hr]). Slagging furnace internal dimensions are 47 in. (119 cm) in diameter by roughly 16 ft (4.9 m) in total length.

The vertically oriented furnace shell was designed to include four distinct furnace sections. The top section of the furnace supports the main burner connection, while the upper-middle furnace section provides a location for installation of the RAH panels. The lower-middle furnace section supports the auxiliary gas burner; the bottom section of the furnace includes the furnace exit to the slag screen as well as the slag tap opening. Flue gas temperature measurements are made using two Type S thermocouples protruding 1 in. (2.5 cm) into the furnace through the refractory wall and three optical pyrometers (flame, flue gas along the furnace wall near the RAH panel, and flue gas at the furnace exit). Furnace temperature is also measured using thermocouples located at the interface between the high-density and intermediate refractory layers as well as between the intermediate and insulating refractory layers. A pressure transmitter and gauges are used to monitor static pressures in order to monitor furnace performance. These data (temperatures and pressures) are automatically logged into the data acquisition system and recorded manually on data sheets on a periodic basis as backup.

The slag tap is intended to be as simple and functional as possible. To that end, the design is a simple refractory-lined hole in the bottom of the furnace. The diameter of the slag tap is nominally 4 in. (10 cm), with a well-defined drip edge. A two-port natural gas-fired taphole burner is used to maintain slag tap temperature for good slag flow. To minimize heat losses, slag is collected in an uncooled, dry container with refractory walls. When the slag tap had plugged in the first couple years of the project, the plug was typically removed on-line after a switch was made to natural gas firing for a short period of time (2 hours) in the main burner. In the last 9 months, an approach has been developed and personnel safety equipment acquired to permit the removal of slag tap plugs on-line while coal is fired. During the December test period, the slag tap did not plug. However, the slag tap was cleaned on-line once in December to prevent a potential plug.

The refractory walls in the slagging furnace are composed of three layers of castable refractory. They consist of an inner 4-in. (10.2-cm) layer of high-density (14-Btu-in./ft²°F-hr, or 2.0-W/m-K) slag-resistant material, 4 in. (10.2 cm) of an intermediate refractory (4.0 Btu-in./ft²°F-hr, or 0.6 W/m-K), and a 3.25-in. (8.3-cm) outer layer of a low-density insulating refractory (1.3 Btu-in./ft²°F-hr, or 0.2 W/m-K). Three refractory layers were selected as a cost-effective approach to keeping the overall size and weight of the furnace to a minimum while reducing slag corrosion and heat loss. Table 2-1 summarizes properties for refractory material used in the SFS. The condition of the high-density refractory in all sections of the furnace appeared to be good following the test completed in December 1999.

Main and Auxiliary Burners

The main burner is natural gas- and pulverized fuel-capable. The basic design is an International Flame Research Foundation (IFRF)-type adjustable secondary air swirl generator, which uses primary and secondary air at approximately 15% and 85% of the total air, respectively, to adjust swirl.

Increasing swirl to provide flame stability and increased carbon conversion can also affect the formation of NO_x. Carbon conversion has been >99% when bituminous and subbituminous coal and lignite are fired. High carbon conversions can be obtained at low swirl settings because of the high operating temperature and adequate residence time. Combustion air flow rates through the main burner range from about 400 to 600 scfm (11 to 17 m³/min), depending on the furnace firing rate and the fuel type (bituminous, subbituminous, or lignite).

An auxiliary gas burner (maximum firing rate of 850,000 Btu/hr, or 896,750 kJ/hr) is located near the furnace exit to control furnace exit temperature, ensuring desired slag flow from the furnace and the slag screen. This auxiliary burner is used to compensate for heat losses through the furnace walls, sight ports, and RAH test panel. Use of the auxiliary gas burner is beneficial during start-up to reduce heatup time and to prevent slag from freezing on the slag screen when the switch is initially made to coal firing.

Table 2-1
Refractory Properties

| Refractory: | Plicast Cement-Free 99V KK/99V ¹ | Plicast Cement-Free 98V KK/98V ¹ | Plicast Cement-Free 96V KK/96V ¹ | Narco Cast 60 | Plicast LWI-28 | Plicast LWI-20 | Harbison-Walker 26 |
|---|--|--|--|------------------|-------------------|-------------------|--------------------|
| Function | High density | High density | High density | High density | Insulating | Insulating | Insulating |
| Service Limit, °F | 3400 | 3400 | 3300 | 3100 | 2800 | 2000 | 2600 |
| Density, lb/ft ³ | 185 | 185 | 185 | 145 | 80 | 55 | 66 |
| K, Btu-in./ft ² °F-hr @ 2000°F | 14.5 | 14.5 | 14.0 | 6.5 | 4.0 | NA ² | 2.2 |
| K, Btu-in./ft ² °F-hr @ 1500°F | 14.7 | 14.7 | 14.2 | 6.0 | 3.0 | 1.7 | 1.9 |
| K, Btu-in./ft ² °F-hr @ 1000°F | 15.5 | 15.5 | 15.0 | 5.6 | 2.7 | 1.3 | 1.7 |
| Hot MOR ³ @ 2500°F, psi | 650 | 750 | 1400 | NA | NA | NA | NA |
| Hot MOR @ 1500°F, psi | — | — | 2000 | 1000 | 250 | 100 | 110 |
| Cold Crush Strength @ 1500°F, psi | — | — | 10000 | NA | 750 | 400 | 350 |
| Typical Chemical Analysis, wt% (calcined) | | | | | | | |
| Al ₂ O ₃ | 99.6 | 98.6 | 95.5 | 62.2 | 54.2 | 39.6 | 53.8 |
| SiO ₂ | 0.1 | 1.0 | 3.8 | 28.0 | 36.3 | 31.5 | 36.3 |
| Fe ₂ O ₃ | 0.1 | 0.1 | 0.1 | 1.0 | 0.8 | 5.4 | 0.5 |
| TiO ₂ | 0.0 | 0.0 | 0.0 | 1.7 | 0.5 | 1.5 | 0.6 |
| CaO | 0.1 | 0.1 | 0.1 | 2.8 | 5.7 | 19.5 | 7.2 |
| MgO | 0.0 | 0.0 | 0.0 | 0.1 | 0.2 | 0.8 | 0.2 |
| Alkalies | 0.2 | 0.2 | 0.2 | 0.2 | 1.5 | 1.4 | 1.4 |

¹ The “KK” designation indicates the presence of fibers that promote dewatering during curing.

² Not applicable.

³ Modulus of rupture.

Radiant Air Heater Panel

A key design feature of the furnace is accessibility for installation and testing of an RAH panel. The furnace will accept a panel with a maximum active size of 1.5×6.4 ft (0.46×1.96 m). This size was selected on the basis of panel-manufacturing constraints identified by UTRC as well as a desire to minimize furnace heat losses. Flame impingement on the RAH panel is not necessarily a problem. Process air for the RAH panel is provided by an EERC air compressor system having a maximum delivery rate of 510 scfm ($14.4 \text{ m}^3/\text{min}$) and a maximum stable delivery pressure of 275 psig (19 bar). Backup process air is available from a smaller compressor at a maximum delivery rate of 300 scfm ($8.5 \text{ m}^3/\text{min}$) and a pressure of <100 psig (<7 bar). A tie-in to a nitrogen system is also available as a backup to the air compressor system. In the event of a failure of inlet process air piping, a backflow emergency piping system was installed so that overheating of the RAH panel could be avoided. UTRC designed and fabricated the RAH test panel.

Slag Screen

The slag screen design for the pilot-scale SFS is the result of a cooperative effort between EERC, UTRC, and PSI personnel. The primary objective for the pilot-scale slag screen is to reduce the concentration of ash particles entering the convective air heater (CAH). The walls of the slag screen consist of two refractory layers. The inner, high-density layer is a Plicast Cement-Free 98V with an outer insulating layer of Harbison-Walker Castable 26. The high-density refractory is 2.25 in. (5.7 cm) thick in the sidewalls and 4 in. (10.2 cm) thick in the roof and floor of the slag screen. The insulating refractory is 3.75 in. (9.5 cm) thick in the sidewalls, roof, and floor. A Plicast LWI-28 refractory was used around the sight ports in the wall of the slag screen. Properties for the high-density and insulating refractory selected for use in the slag screen are summarized in Table 2-1. The current slag screen design permits the use of a maximum of 18 tubes, 1.5 in. (3.8 cm) in diameter, in a six-row staggered array. The number of tubes in use for a given SFS test is dependent on the ash fusion properties of the fuel ash. Water-cooled surfaces were installed inside of the refractory tubes to cool the tubes and reduce the erosion/corrosion observed during shakedown tests. Specific details concerning slag screen modifications and performance this quarter are addressed later in this report.

Dilution/Quench Zone

The dilution/quench zone design was a cooperative effort between the EERC and UTRC. It is refractory-lined and located immediately downstream of the slag screen and upstream of the CAH duct. It is oriented vertically and has a 1.17-ft (0.36-m) inside diameter in the area of the flue gas recirculation (FGR) nozzles, expanding to 2 ft (0.6 m) below the nozzles to provide adequate residence time within duct length constraints. The duct section containing the flue gas recirculation nozzles is a spool piece to accommodate potential changes to the size, number, and orientation of the flue gas recirculation nozzles.

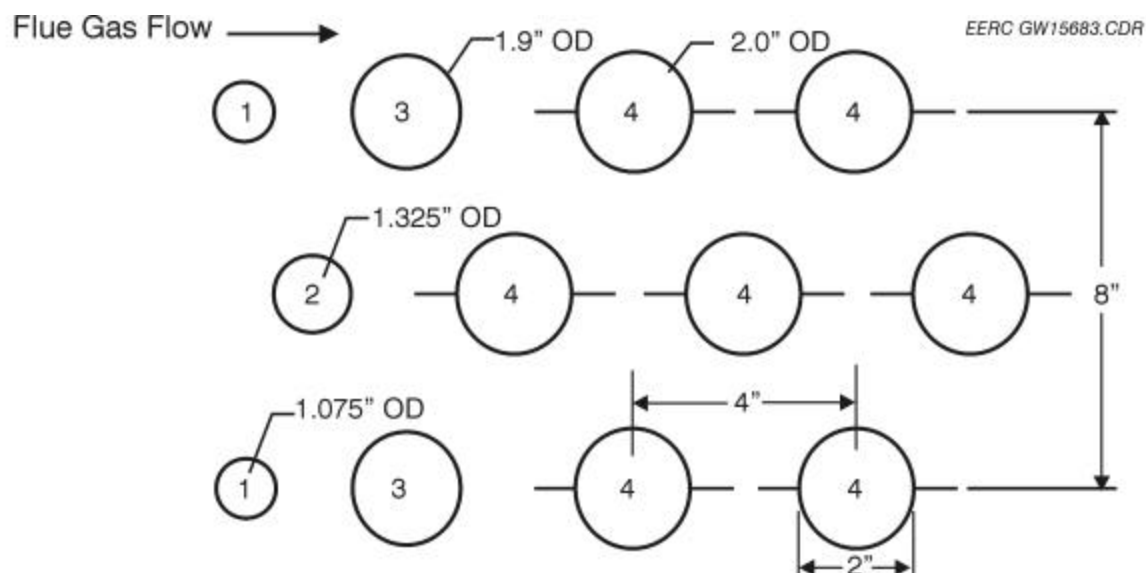
Routine cleaning of the dilution/quench zone has been required during each weeklong bituminous and subbituminous coal-fired test. In order to monitor and document the slag deposition in the dilution/quench zone, a pressure transmitter is used to monitor and record differential pressure. On the basis of observations made during an August 1998 test and the frequent cleaning required, the EERC modified the spool piece section of the dilution/quench zone. The specific modification involved the

addition of a water-cooled wall around the FGR nozzles. This water-cooled wall appears to embrittle the slag deposits that form in this area, making them more prone to spontaneous shedding and generally easier to remove on-line. Performance observations during the December test are summarized later in this report.

Convective Air Heater

The CAH design was a cooperative effort between the EERC and UTRC. The flue gas flow rate to the CAH tube bank has been calculated to range from 3553 to 4619 acfm at 1800°F (101 to 131 m³/min at 982°C). A rectangular inside duct dimension of 1.17 ft² (0.11 m²) results in a flue gas approach velocity of 50 to 73 ft/s (15 to 22 m/s) to the CAH. The CAH originally consisted of twelve 2-in. (5-cm)-diameter tubes installed in a staggered three-row array. The first five tubes in the flue gas path were uncooled ceramic material, with the remaining seven tubes cooled by heated process air. The uncooled ceramic tubes were replaced in May 1998 with uncooled stainless steel tubes because the ceramic tubes were repeatedly damaged when the tube bank was removed from the duct.

In September 1998, the uncooled tubes were again replaced. The replacement tubes represented three high-temperature alloy types (Incoloy MA956, Incoloy MA956HT, and PM2000) and three pipe sizes (1.5-in. [3.8-cm] Schedule 80, 1-in. [2.5-cm] Schedule 40, and 0.75-in. [1.9-cm] Schedule 40, respectively). Exhibit 2-2 illustrates the original position, size, and alloy type for the five uncooled tubes. At the request of UTRC, two of these uncooled alloy tubes were removed from the CAH tube bank following the September 1999 test and returned to UTRC for characterization. The tubes removed from the CAH represent the alloys designated Incoloy MA956HT and Incoloy MA956. Replacement tubes were fabricated using 1.5 in. (3.8 cm) Schedule 40 stainless steel pipe prior to the December 1999 test. No additional changes were made to the CAH this past quarter.



¹Uncooled, PM 2000 (nominally 0.75-in. Schedule 40 pipe).

²Replaced prior to December test, using 1.5-in. Schedule 40 stainless steel pipe.

Uncooled, Incoloy Alloy MA956HT (nominally 1-in. Schedule 40 pipe).

³One tube replaced prior to December test, using 1.5-in. Schedule 40 stainless steel pipe.
Uncooled, Incoloy Alloy MA956 (1.5-in. Schedule 80 pipe).

⁴Air-cooled, Inconel 625 (2-in. tubing, 0.188-in. Wall).

Exhibit 2-2
Illustration of the Tubes in the CAH Tube Bank

Emission Control

A pulse-jet baghouse is used for final particulate control on the pilot-scale SFS. The baghouse design permits operation at both cold-side (250° to 400°F, 121° to 205°C) and hot-side (600° to 700°F, 316° to 371°C) temperatures. The primary baghouse chamber and ash hopper walls are electrically heated and insulated to provide adequate temperature control to minimize heat loss and avoid condensation problems on start-up and shutdown. The main baghouse chamber was designed with internal angle iron supports to handle a negative static pressure of 20 in. W.C. (37 mm Hg).

During the past quarter, the tube sheet used permitted the installation of 36 bags arranged in a six-by-six array. Bag dimensions are nominally 6 in. (15.2 cm) in diameter by 10 ft (3.0 m) in length, providing a total filtration area of (565 ft² [52.5 m²]). The bag type being used at this time is a 22-oz/yd² (747-g/m²) woven glass bag with a polytetrafluoroethylene (PTFE) membrane. Pulse cleaning of the bags was accomplished on-line in December using a reservoir pulse-air pressure of nominally 60 psig (4.1 bar). Baghouse performance observations during the December test are summarized later in this report.

Instrumentation and Data Acquisition

The instrumentation and data acquisition components for the pilot-scale SFS address combustion air, flue gas, process air, process water, temperatures, static and differential pressures, and flow rates. The data acquisition system is based on a Genesis software package and three personal computers.

Two sets of flue gas instrumentation (oxygen, carbon dioxide, carbon monoxide, sulfur dioxide, and nitrogen species) are dedicated to support the operation of the SFS. Flue gas is transferred from the sample point through a heated filter and sample line to the sample conditioner before it reaches the analyzers. Flue gas is routinely sampled in the slag screen at the furnace exit and the exit of the baghouse. Total flue gas flow rate through the SFS is measured using a venturi. No instrumentation work was completed this past quarter other than routine maintenance and calibration.

Pilot-Scale SFS Activities This Quarter

The pilot-scale SFS was fired on natural gas (heatup and cooldown) and an Illinois No. 6 bituminous coal for 202 hours during the period December 12–23 (SFS-RH11-0799). Because the results from that test were not available for inclusion in the October through December quarterly report, they are presented here. The purpose was to evaluate the new Kyocera tile installed in early December, as well as the effectiveness of a sootblowing capability added to the CAH. Data evaluation and sample analysis have been completed. Therefore, this report summarizes the results and observations for the December test as well as SFS maintenance and modification activities this past quarter. In addition, a 200-hr subbituminous coal-fired SFS test was completed in March. In comparison to an earlier subbituminous coal test, the March test was performed to test the corrosion resistance of the Kyocera tile to subbituminous coal slag, determine the effects of increased cooling of slag screen tubes on slag screen preservation, measure the performance of the CAH with finned tubes, and determine if CAH deposits can be cleaned by sootblowing. However, results from that test are not available for inclusion in this report and will be summarized in a subsequent quarterly report.

The December 1999 SFS test was terminated after completion of 202 hr of a planned 200-hr coal-fired test. Coal firing was terminated, and natural gas firing was initiated and continued for 4 hr to maintain furnace operating temperature (2800°F/1538°C) and minimize the quantity of residual slag on the RAH tile surfaces and in the slag screen and slag tap. After 4 hr of natural gas firing, stepwise reductions in the firing rate were made to control cooldown at a rate of <100°F/hr (38°C/hr). Natural gas firing was discontinued once the furnace temperature reached 1500°F (816°C). At that point, air flow rates were reduced to minimums, and the SFS was allowed to cool down slowly for a few days before the top section of the furnace was removed to permit inspection of the RAH panel.

Fuel Feed System

Nominal feed rates during the December test were 170 to 185 lb/hr (77 to 84 kg/hr). Adjustments to coal feed rate were made in order to maintain a flue gas temperature near the RAH tile surfaces and furnace exit of 2800°F (1538°C). Coal feed was continuous except for a 2-hr natural gas-fired period required to clean out the ash/slag pot below the dilution/quench zone after roughly 160 hr of coal firing. Removal of ash/slag from this location was necessary to avoid a potential plugging problem and a possible forced shutdown. The slag pot below the slag tap was changed once during the December test as planned with no interruption of coal feed. Exhibit 2-3 illustrates the coal feed rate data for the December test. During the test, the coal feed rate was quite stable except for a few minor spikes (high and low) associated with coal-hopper refill cycles.

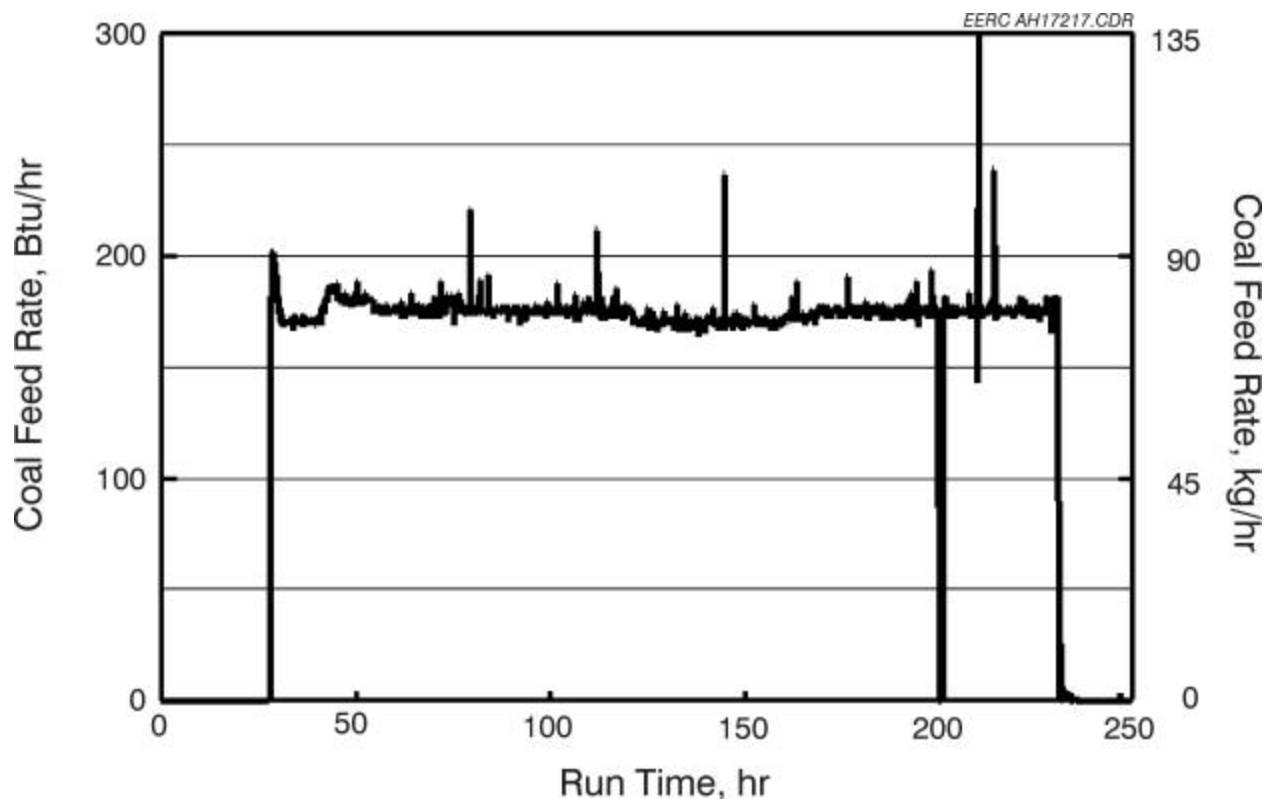


Exhibit 2-3

Coal Feed Rate Versus Run Time for the December Test, SFS-RH11-0799

Tables 2-2 and 2-3 summarize analytical results for all of the coals that had been fired in the SFS through December 1999. They include Illinois No. 6 bituminous, Kentucky bituminous, Prater Creek bituminous, and Rochelle subbituminous coals and Coal Creek Station (CCS) and Milton R. Young Station (MRYS) lignites. The analyses of the composite Illinois No. 6 coal fired in December indicated that the as-fired fuel contained 2.8–3.2 wt% moisture, 11.0–11.7 wt% ash, and 3.3–3.5 wt% sulfur. The heating value was 11,554–11,627 Btu/lb (26,849–27,019 kJ/kg) on an as-fired basis. These data are essentially the same as the data resulting from previous SFS tests firing Illinois No. 6 coal. The only exception is the slightly lower fuel moisture content, 2.8–3.2 versus 4.4–10.3 wt%. Coal ash was analyzed for ash fusion properties under oxidizing conditions. Results indicate a softening temperature of 2417°F (1325°C) and a fluid temperature of 2590°F (1421°C). The fluid temperature of this coal ash was roughly 60°F (33°C) higher when compared to the analyses of the Illinois No. 6 fuel previously fired. However, slag screen and slag tap plugging were avoided using temperature control and one on-line preemptive cleaning of the slag tap.

Dry-sieve analysis indicated that the pulverized Illinois No. 6 coal was nominally 74–77 wt% !200 mesh (74 microns [μm]) in December. This is a smaller size distribution than was observed for the bituminous coals fired in the second and third quarters of 1999 and consistent with the desired size distribution, 70 wt% ≤200 mesh (74 μm). The improvement in pulverization efficiency is believed to be the result of hammer replacement and careful attention to hammer balance. The carbon content of the fly ash collected in the baghouse was 0.10 wt%, indicating excellent combustion efficiency during the December test.

X-ray fluorescence (XRF) analysis results for the various ashed fuels are summarized in Tables 2-2 and 2-3 and reported as oxides. The Illinois No. 6 coal fired in December was nearly identical to the Illinois No. 6 coal fired during several previous SFS tests in terms of ash analyses. However, the ash fusion temperatures were the highest in the ranges shown in Table 2-2 for the Illinois No. 6 fuels. The impacts of the higher ash fusion properties/temperatures on the performance of the slag screen and slag tap are discussed later in this report.

Table 2-2
Results of Coal and Coal Ash Analysis for Coal-Fired Slagging Furnace Tests¹

| | Illinois No. 6 Bituminous Coal | Kentucky Bituminous Coal | Prater Creek Bituminous Coal | Rochelle Subbituminous Coal |
|--------------------------------|-----------------------------------|-----------------------------|---------------------------------|--------------------------------|
| Proximate Analysis, wt% | | | | |
| Moisture | 2.8–10.3 | 2.3–2.5 | 2.0 | 21.6–24.3 |
| Volatile Matter | 35.9–39.9 | 38.2–38.7 | 38.7 | 35.6–37.4 |
| Fixed Carbon | 43.3–46.3 | 54.7–54.9 | 54.5 | 35.8–36.7 |
| Ash | 10.6–11.7 | 3.9–4.7 | 4.7 | 4.3–4.7 |
| Ultimate Analysis, wt% | | | | |
| Hydrogen | 4.7–5.8 | 5.2–5.5 | 5.4 | 6.1–6.4 |
| Carbon | 61.6–67.6 | 77.5–78.2 | 78.3 | 53.0–55.2 |
| Nitrogen | 0.8–1.9 | 1.8 | 2.3 | 0.6–0.7 |
| Sulfur | 3.2–4.1 | 0.8–1.0 | 0.8 | 0.3 |
| Oxygen | 10.6–17.6 | 9.6–9.7 | 8.4 | 32.9–33.4 |
| Ash | 10.6–11.7 | 3.9–4.7 | 4.7 | 4.3–4.7 |
| Heating Value, Btu/lb | | | | |
| | 11,015–11,658 | 13,861– 14,120 | 14,167 | 9021–9328 |
| Percent as Oxides, wt% | | | | |
| SiO ₂ | 49.3–53.9 | 42.5–44.8 | 38.4 | 26.7–27.1 |
| Al ₂ O ₃ | 19.8–21.5 | 28.9–29.8 | 25.0 | 15.5–16.3 |
| Fe ₂ O ₃ | 13.6–17.5 | 13.7–14.5 | 22.5 | 6.3–6.6 |
| TiO ₂ | 0.9–1.0 | 1.1 | 1.0 | 1.2–1.4 |
| P ₂ O ₅ | 0.1–0.2 | 0.1 | 0.1 | 0.7–0.9 |
| CaO | 2.6–3.6 | 1.9–2.8 | 3.8 | 21.6–24.3 |
| MgO | 1.5–2.0 | 2.2–2.4 | 2.1 | 6.7–6.9 |
| Na ₂ O | 1.1–1.5 | 1.1–1.3 | 0.3 | 1.5 |
| K ₂ O | 1.9–2.3 | 2.7–3.0 | 2.2 | 0.1–0.4 |
| SO ₃ | 2.5–4.0 | 2.4–3.8 | 4.6 | 15.6–17.0 |
| Ash Fusion Temp., °F | | | | |
| Initial | 2315–2392 | 2398–2577 | 2483 | 2202–2295 |
| Softening | 2342–2418 | 2440–2603 | 2490 | 2205–2308 |
| Hemisphere | 2392–2448 | 2474–2621 | 2544 | 2214–2311 |
| Fluid | 2491–2593 | 2588–2684 | 2593 | 2221–2325 |
| Sieve Analysis | | | | |
| Screen Mesh Size | Weight Percent Retained | | | |
| 100 | 1.8–25.2 | 8.1–11.4 | 13.6 | 7.6–8.8 |
| 140 | 0–14.9 | 12.9–13.9 | 15.1 | 14.2–15.4 |
| 170 | 0–14.9 | NA ² | NA | NA |
| 200 | 9.6–13.5 | 11.4–13.5 | 12.4 | 14.3–14.4 |
| 230 | 0–16.2 | 8.7–9.4 | 8.3 | 8.4–9.1 |
| 270 | 0.5–14.6 | 0.7–1.6 | 0.8 | 2.0–5.6 |
| 325 | 7.4–14.7 | 11.9–12.7 | 10.9 | 4.8–11.6 |
| 400 | 0–4.7 | NA | NA | NA |
| Pan | 29.7–57.8 | 41.2–42.6 | 38.8 | 39.7–43.4 |
| Total % | 99–100.2 | 99.9–100.1 | 99.9 | 98.6–100.6 |

¹ As-fired basis.

Table 2-3
Analysis of Lignite and Lignite Ash Slagging Furnace Tests¹

| | Coal Creek Station Lignite | Milton R. Young Station Lignite |
|--------------------------------|----------------------------|---------------------------------|
| Proximate Analysis, wt% | | |
| Moisture | 31.6–37.9 | 33.8–37.1 |
| Volatile Matter | 29.4–31.5 | 30.4–32.1 |
| Fixed Carbon | 26.4–26.8 | 26.9–27.9 |
| Ash | 6.3–10.2 | 5.6–6.2 |
| Ultimate Analysis, wt% | | |
| Hydrogen | 6.4–6.8 | 7.0–7.2 |
| Carbon | 38.5–40.9 | 41.1–43.4 |
| Nitrogen | 0.6 | 0.6 |
| Sulfur | 0.5–0.7 | 0.7–0.9 |
| Oxygen | 41.1–47.3 | 42.1–44.9 |
| Ash | 6.3–10.2 | 5.6–6.2 |
| Heating Value, Btu/lb | 6300–6708 | 6933–7144 |
| Percent as Oxides, wt% | | |
| SiO ₂ | 31.8–35.5 | 11.2 |
| Al ₂ O ₃ | 11.7–12.0 | 8.6 |
| Fe ₂ O ₃ | 6.4–8.0 | 13.2 |
| TiO ₂ | 0.5 | 0.2 |
| P ₂ O ₅ | 0.3 | 0.1 |
| CaO | 17.0–18.7 | 21.3 |
| MgO | 6.5–7.0 | 7.3 |
| Na ₂ O | 2.9–3.2 | 11.7 |
| K ₂ O | 1.3 | 0.2 |
| SO ₃ | 16.0–19.0 | 26.2 |
| Ash Fusion Temp., °F | | |
| Initial | 2170–2188 | 2370–2371 |
| Softening | 2181–2196 | 2381–2384 |
| Hemisphere | 2189–2203 | 2384–2387 |
| Fluid | 2196–2219 | 2392–2428 |
| Sieve Analysis | | |
| Screen Mesh Size | Weight Percent Retained | |
| 100 | 6.4–10.3 | 14.9 |
| 140 | 12.3–13.8 | 15.7 |
| 170 | NA ² | 4.6 |
| 200 | 11.9–12.3 | 8.5 |
| 230 | 3.7–8.5 | NA |
| 270 | 6.2–10.2 | 3.1 |
| 325 | 6.4–6.5 | 14.9 |
| 400 | NA | NA |
| Pan | 41.5–48.2 | 38.2 |
| Total % | 98.3–99.9 | 99.9 |

¹ Lignite analysis is presented on an as-fired basis.

² Not available.

Slagging Furnace Operation

The slagging furnace heating rate during the December test period was limited to 100°F/hr (56°C/hr) while natural gas was fired, as recommended for the RAH panel by UTRC. When the furnace reached normal operating temperature (2800°F, 1538°C), the main burner was switched from natural gas to coal firing. The coal-firing rate was nominally 2.0 MMBtu/hr (2.1×10^6 kJ/hr) with an auxiliary burner firing rate of 0.5 to 0.55 MMBtu/hr (0.53 to 0.58×10^6 kJ/hr). These coal-firing conditions were maintained for 202 hr in an attempt to maintain a furnace flue gas temperature near the RAH panel of 2800°F (1538°C). This temperature measurement was made using an optical pyrometer with secondary measurements using Type S thermocouples. A summary of furnace and slag screen temperatures is presented as a function of run time in Exhibit 2-4. Corresponding slagging furnace firing rate data are summarized in Exhibit 2-5.

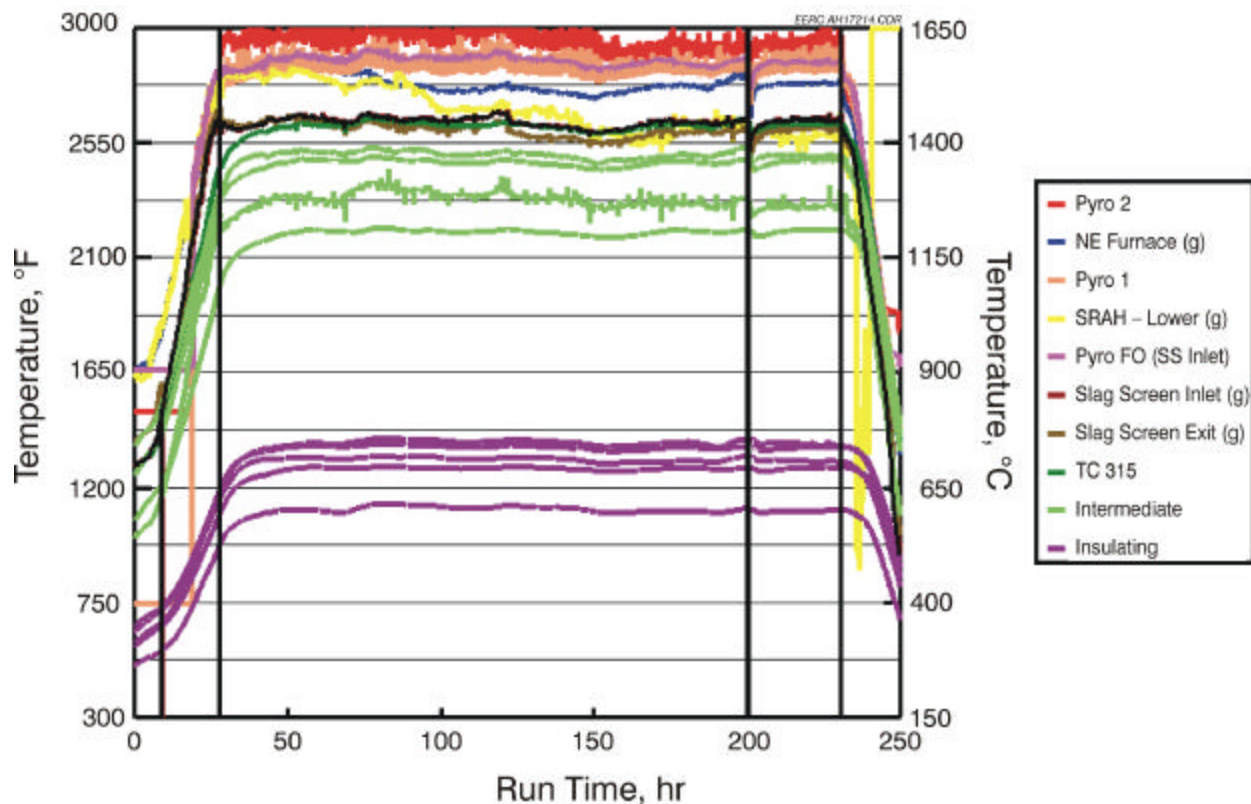


Exhibit 2-4

Furnace and Slag Screen Temperatures Versus Run Time for the December Test, SFS-RH11-0799

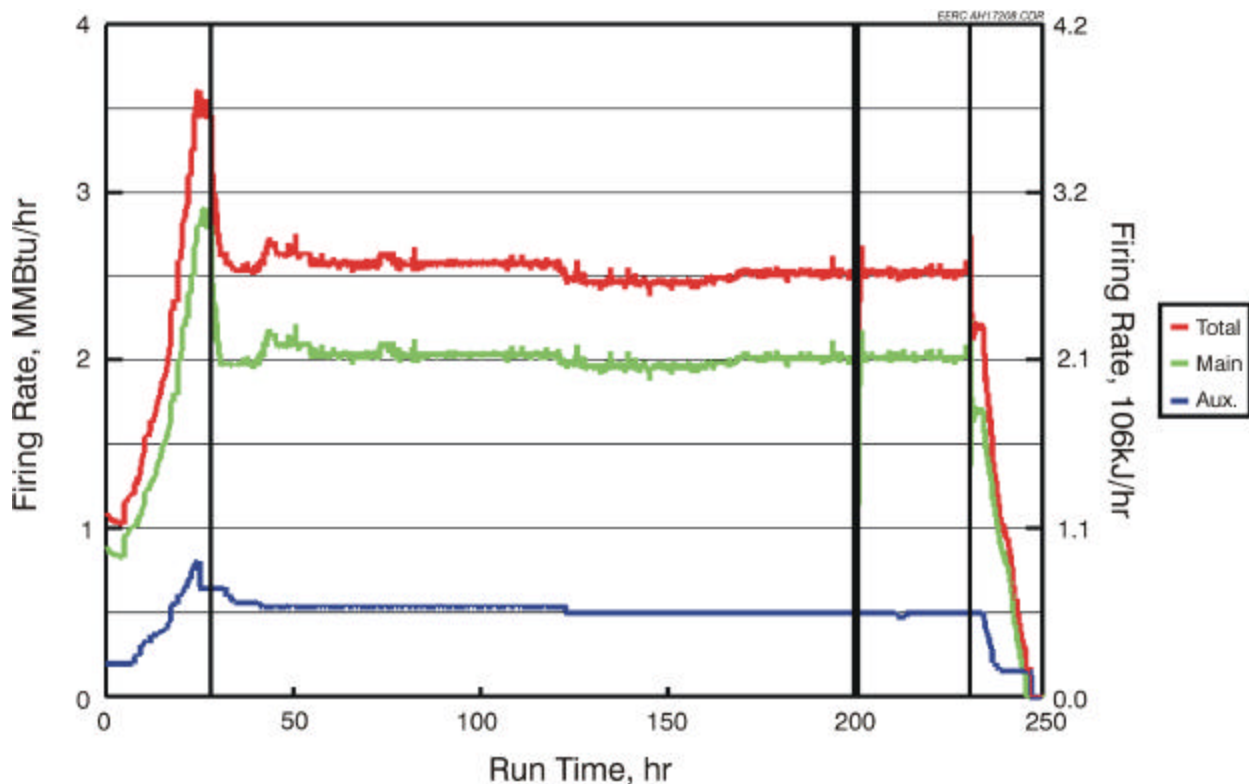


Exhibit 2-5

Slagging Furnace Firing Rate Versus Run Time for the December Test, SFS-RH11-0799

The total furnace-firing rate (main plus auxiliary burners) ranged from 2.5 to 2.6 MMBtu/hr (2.6 to 2.7×10^6 kJ/hr). The main burner-firing rate ranged from 2.0 to 2.1 MMBtu/hr (2.1 to 2.2×10^6 kJ/hr), accounting for about 80% of the total energy input. The resulting flue gas temperature near the furnace wall/RAH panel and furnace exit was 2795° to 2865°F (1535° to 1574°C).

Furnace refractory temperatures ranged from 1130° to 1395°F (610° to 758°C) for the hot side of the insulating refractory to as high as 2520°F (1382°C) for the cold side of the high-density refractory. Compared to the May 1999 test period firing Illinois No. 6 coal, the insulating refractory temperatures were 50° to 65°F (28° to 36°C) higher, and high-density refractory temperatures were 40°F (22°C) higher. These higher refractory temperatures were observed even though the total furnace firing rate in December was 4% to 5% lower than the firing rate in May. In addition, the main burner firing rate in December was 9% lower than that required in May, 2.0 to 2.1 MMBtu/hr (2.1 to 2.2×10^6 kJ/hr) versus 2.25 to 2.3 MMBtu/hr (2.2 to 2.4×10^6 kJ/hr), but resulted in 20° to 35°F (11° to 19°C) higher furnace temperatures. The higher furnace temperatures achieved in December with a lower firing rate were most likely the result of a lower fuel moisture content, nominally 3 wt% in December versus 5 wt% in May.

The high-density refractory lining the furnace was found to be in good condition following the December test. The slag screen inlet, with rounded edges on the sides, continues to show minimal erosion. However, as a result of high-density refractory thermal shrinkage during furnace cooling, two

pieces of castable refractory above the RAH panel were slightly damaged when they became wedged against the castable refractory block above the RAH panel and could not move with the high-density refractory liner. These pieces slipped into their proper position when the surfaces were pried apart, and the cracks were patched using the same castable material. Exhibit 2-6 presents a photograph of the interior of the furnace showing the refractory damage above and left and right of the RAH panel and the RAH panel following the December test. Although not obvious in the photograph, the high-density refractory liner in the furnace is continuing to darken with each coal-firing period.



Exhibit 2-6

Photograph of Furnace Interior Following the December Test, SFS-RH11-0799

Main and Auxiliary Burners

The main and auxiliary burners performed well during the December test. As previously stated, the main burner swirl was maintained at about 20%, while the auxiliary burner swirl setting was 80%–100%. Carbon efficiency for the Illinois No. 6 bituminous coal was >99.99% because of the high furnace operating temperature and residence time. Based on operating experience, the EERC intends to continue minimum main burner swirl as necessary to establish a stable flame in order to establish uniform temperatures over the length of the furnace and minimize NO_x emissions. Auxiliary burner firing is adjusted as necessary to maintain desired slag screen inlet temperatures, but will be minimized whenever possible.

Slag Screen

No changes were made to the slag screen between the September and December tests; the slag screen configuration included three rows of three tubes each. Although the slag screen tubes in the first row had been eroded during the September test to a diameter of roughly 1 in. (2.5 cm), the tubes were intact and replacement was not necessary. Consistent with previous slag screen operating experience, the second and third rows of tubes were eroded to a lesser degree than the first row. Measured slag screen flue gas temperatures during the December test were typically 2580° to 2655°F (1416° to 1458 °C) at the inlet and 2550° to 2615°F (1399° to 1435°C) at the outlet. These measured temperatures are believed to be less than the actual flue gas temperatures because the thermocouple is behind individual water-cooled slag screen tubes and because of observed thermocouple deterioration by slag attack. Therefore, slag screen temperature control is based on an optical pyrometer measurement at the furnace exit/slag screen inlet. Based on the pyrometer temperature measurement, flue gas entering the slag screen was nominally 2800°F (1538°C). Slag screen operating temperature is selected on the basis of ash fusion data for the fuel to be fired. The EERC tries to operate the slag screen at flue gas temperatures of 100° to 200°F (56° to 112°C) above the fluid temperature of the fuel ash to ensure slag flow from the slag screen to the slag tap. The ash fluid temperature (under oxidizing conditions) of the composite sample of Illinois No. 6 coal analyzed following the December test period was determined to be 2590°F (1421°C).

Slag screen plugging and differential pressure control problems were not encountered when Illinois No. 6 coal was fired during the December test. Therefore, no limestone or other additive injection was necessary to facilitate operation. The slag tap did not plug during the December test. However, the slag tap was cleaned on-line once to avoid a potential plug. Slag tap temperature was controlled at 2640° to 2740°F (1449° to 1505°C) using the natural gas-fired tap burners. The slag pot was changed once during the December test as planned because of slag accumulation. Ash fusion analysis of slag samples collected following the December test determined that the fluid temperature of the slag (in an oxidizing environment) was 2580°F (1416°C). XRF analysis showed some enrichment of the iron concentration along with depletion of alkali components.

Exhibit 2-7 is a photograph of the slag screen inlet following the December test. All three rows of slag screen tubes experienced an additional loss in mass, measuring only about 0.75 in. (1.9 cm) in diameter at the smallest point, from a starting diameter of 1 in. (2.5 cm) prior to the December test.



Exhibit 2-7

Photograph of the Slag Screen Inlet Following the December Test, SFS-RH11-0799

Based on previous experience, successful slag screen performance during the subbituminous coal-fired test planned for March required eighteen water-cooled tubes in the slag screen. Therefore, the slag screen was rebuilt in January 2000 allowing for the installation of eighteen water-cooled stainless steel tubes (six rows of three) covered with high-density alumina refractory resulting in an outside diameter of 1.5 in. (3.8 cm). The first rows of tubes were fabricated using 0.5-in. (1.3-cm) stainless steel tubing, with the second and third rows fabricated using 0.38-in. (0.95-cm) stainless steel tubing. The remaining three rows of tubes were fabricated using 0.25-in. (0.64-cm) stainless steel tubing. The use of three different water-cooled tubing sizes was intended to maximize cooling to the rows most prone to erosion/corrosion and limit the potential for plugging in the slag screen.

In February, the new refractory in the slag screen was cured at temperature hold points through 650°F (344°C). Following the refractory curing in February, some minor refractory damage was noted and repaired. Final curing of the slag screen refractory occurred during SFS heatup at the beginning of the SFS test in March.

Following the December test, slag and ash samples from system components and piping were collected and weighed in order to prepare a mass balance. A total theoretical ash quantity was calculated (3954 lb or 1795 kg) on the basis of the total coal feed and the measured ash content of the composite coal samples. Total slag and ash recovery from the December test was 81% (3200 lb or 1453 kg). Slag recovery from the furnace, slag pot, and dilution/quench zone represented 56% of the theoretical ash. Additional slag is evident on the furnace wall, on the RAH panel, in the bottom of the

furnace, in the slag screen, and in the upper section of the dilution/quench zone. However, this material is not recoverable from the high-density refractory.

Fly ash recovered from other system components (drawdown gas line, CAH duct, process air preheater tubes, tube-and-shell heat exchangers, cyclone, baghouse, and flue gas piping) represented 25% of the theoretical ash for the December test. Nominally 10% to 15% of the ash in the fuels fired in the SFS has been reaching the baghouse. In December, that value was 16% of the total ash/slag.

Dilution/Quench Zone

Slag deposits formed in the vicinity of the FGR nozzles during the September test. As a result, it was necessary to clean the area of the FGR nozzles on a periodic basis. The dilution/quench zone was initially cleaned after 11 hours of coal firing. During the December test, cleaning frequency (2–4 hr) after roughly 40 hr of coal firing was dependent on differential pressure in the quench zone. About 23% of the ash/slag recovered from the SFS was recovered in the dilution/quench zone. This quantity of material is greater when compared to previous tests firing the same fuel. The greater quantity of slag/ash collected in the dilution/quench zone during the December test is believed to be a direct result of the slag screen performance limitations. The reduced diameter of the slag screen tubes as a result of their erosion/corrosion in September and December resulted in a lower slag collection efficiency. Also, when Illinois No. 6 coal is fired, the slag screen has been operated more efficiently using 18 tubes. During future SFS tests firing Illinois No. 6 coal, it would be beneficial to operate the slag screen with 18 tubes. Downstream of the FGR nozzles, the small quantity of ash observed on the refractory walls was weakly sintered.

During the SFS test in December, a small quantity of calcium oxide was injected into the flue gas just upstream of the pulse-jet baghouse. Injecting calcium oxide was an attempt to eliminate the sulfur trioxide that had been observed downstream of the pulse-jet baghouse during previous SFS tests when the Illinois No. 6 coal was fired. However, this effort was only partially successful because of intermittent feeder performance. As a result, 12 ppm of sulfur trioxide was observed downstream of the baghouse, and evidence of acid condensation in the FGR fan and piping was found during maintenance. In fact, the acid condensation degraded the performance of the dilution/quench zone during the last 24–48 hr of SFS operation.

Process Air Preheaters

The process air for the CAH tube bank and the RAH panel is preheated using tube bundles downstream of the CAH. Further heating of the process air entering the RAH panel is achieved electrically. Process air for the CAH tube bank is supplied by the first process air preheater tube bundle. During the December test, process air entering the CAH tube bank was controlled at set points ranging from 1060° to 1100°F (571° to 594°C) for nominal process air flow rates of 90 to 105 scfm (2.5 to 3.0 m³/min). Process air temperatures at the exits of the other four preheater tube bundles were nominally 1180° to 1300°F (638° to 705°C) for combined flow rates totaling 150 to 200 scfm (4.2 to 5.7 m³/min).

Process air preheater temperatures are shown as a function of run time in Exhibit 2-8. Although the process air preheater heat-transfer rate degraded with time as ash deposits developed on the tube

surfaces, process air temperature and flow rate were adequate to support operation of the CAH tube bank and RAH panel.

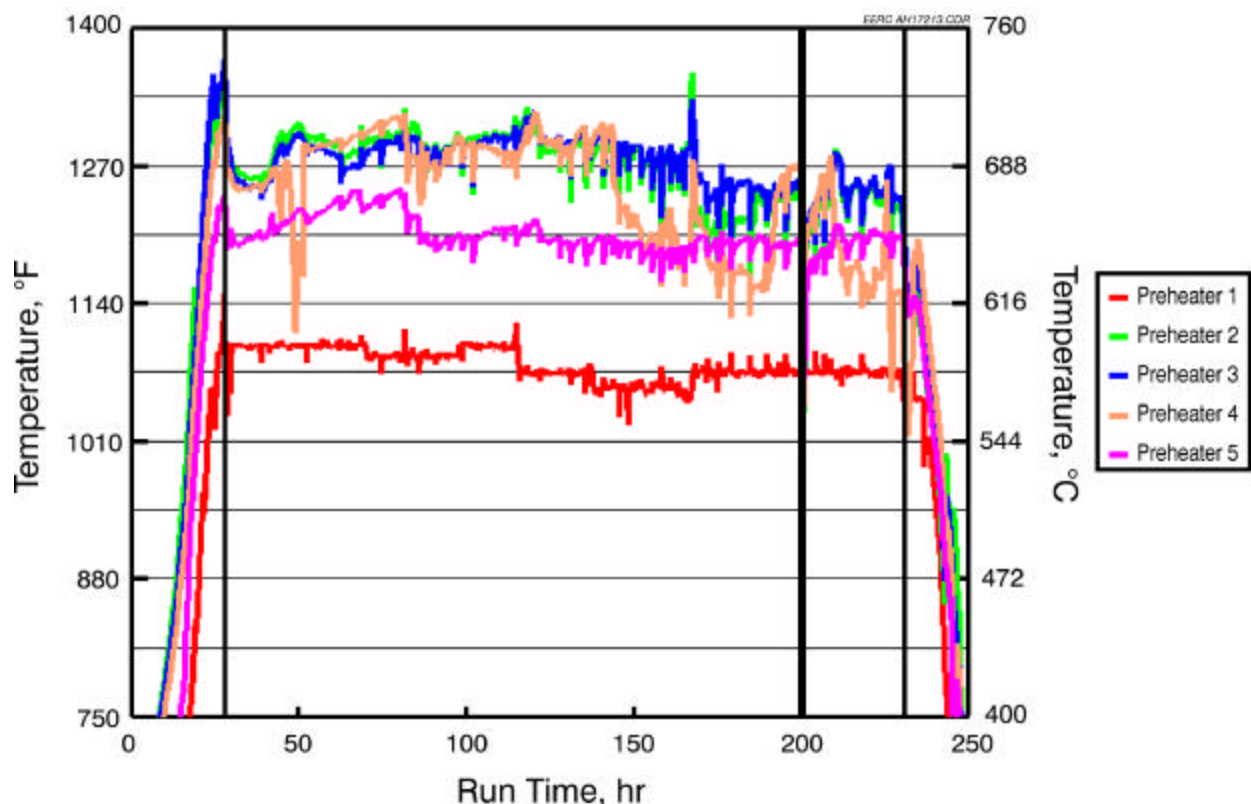


Exhibit 2-8
Process Air Preheater Temperatures Versus Run Time for the December Test,
SFS-RH11-0799

Emission Control

During gas- and coal-fired furnace operation in December, baghouse temperatures and temperature profiles were nominal, and the electrical heaters worked well, limiting the potential for condensation on start-up and shutdown. Baghouse temperature ranged from 325° to 340°F (163° to 171°C). Flue gas flow rates were 880 to 980 scfm (24.9 to 27.8 m³/min). Actual flue gas flow rates through the baghouse were 1379 to 1565 acfm (39.1 to 44.3 m³/min).

The 36 bags (total filtration area of 565 ft² [52.5 m²]) used in the baghouse this past quarter were a 22-oz/yd² (747-g/m²) woven glass with a PTFE membrane. The filter face velocities when the Illinois No. 6 bituminous coal was fired were 2.4 to 2.8 ft/min (0.74 to 0.84 m/min). These filter face velocities are low compared to conventional pulse-jet filtration systems typically operating at or near 4 ft/min (1.2 m/min). However, a detailed evaluation of baghouse performance has not been a specific objective within the scope of work to date.

Measured inlet and outlet particulate mass loadings ranged from 0.0459 to 0.1234 gr/scf (105.1 to 282.6 mg/Nm³) and 0.0002 to 0.0061 gr/scf (0.4580 to 13.97 mg/Nm³), respectively, resulting in

particulate collection efficiencies of 92% to 99.8% in December. The inlet particulate loadings are very similar to those measured when Illinois No. 6 bituminous coal was fired in January and May 1999. In this case, the variability or range of the inlet mass loadings is believed to be the direct result of a variable feed rate observed for a feed system injecting calcium oxide into the flue gas upstream of the pulse-jet baghouse. As previously stated, calcium oxide injection was expected to capture sulfur trioxide in the pulse-jet baghouse to control flue gas sulfur trioxide concentration downstream. However, feed system performance was inconsistent and, therefore, is believed to be responsible for the variability or range of the measured particulate mass loadings at the outlet of the pulse-jet baghouse. Higher outlet mass loadings are believed to be the result of sulfur trioxide condensation in the sample train based on visual observations concerning the probe and filter.

Calculated particulate emissions from the pulse-jet baghouse ranged from 0.0008 to 0.0233 lb/MMBtu. The low end of the range represents a sampling period when the calcium oxide injection system was working properly, with the high end of the range believed to represent a sampling period when calcium oxide injection was not occurring. Although the range in measured particulate emissions represents nearly a factor of 30, the data are generally comparable to emission rates previously measured when other coals and lignite (0.0004 to 0.0074 lb/MMBtu) were fired in the SFS. Visual inspection of the outlet filters resulting from December sampling indicated possible acid condensation on three of the four filters. Evidence of acid condensation was found in the corners of the clean air plenum of the pulse-jet baghouse and downstream flue gas piping after the December test as a function of routine maintenance.

Two sulfur trioxide concentration measurements were made downstream of the pulse-jet baghouse in December. These measurements indicated that the sulfur trioxide concentration at this location was 11–13 ppm. This value is lower than the 45 ppm value measured in April 1999 when Illinois No. 6 coal was fired without calcium oxide injection, yet higher than the 4 ppm value measured in May 1999 when a calcium oxide injection rate of 0.5 lb/hr (227 g/hr) was successfully used to limit the sulfur trioxide concentration downstream of the pulse-jet baghouse.

In addition to the standard EPA Method 5 sampling completed in December, respirable mass emissions (defined below) were measured at the outlet of the pulse-jet baghouse using a TSI Inc. aerodynamic particle sizer (APS-33). This real-time measurement method measures particle mass in the range of 0.5 to 15 μm . The primary advantages of this system are the high spatial resolution and the short sampling time. In the APS-33, particle-laden air is passed through a thin-walled orifice, with the particles lagging behind the gas because of their higher inertia. This lag allows the determination of the aerodynamic diameter of a particle by measuring its velocity as it exits from the orifice. To measure the particle velocity, the APS-33 employs a laser beam split in two and refocused onto two rectangular planes a set distance apart in front of the orifice. The light scattered by a particle passing through these beams is collected and focused onto a photomultiplier tube, which emits two pulses separated by the time taken for the particle to cross the distance between the two planes. This time interval is measured electronically and used to calculate the particle's aerodynamic diameter.

Respirable mass is a calculated value defined by the American Council of Governmental and Industrial Hygienists for particles in the aerodynamic size range of 2 to <10 μm . Exhibit 2-9 presents the respirable mass emissions data for the December test period. The data are presented on a mg/m^3 basis

versus sampling time. The respirable mass emission rate was nominally 0.003 mg/m^3 based on integrated averages during the two sampling periods, with the first sampling period being somewhat lower and the second somewhat higher. Emission spikes as a function of cleaning cycles showed a similar trend, with spikes approaching 0.02 mg/m^3 observed during the first sampling period and spikes approaching 0.06 mg/m^3 during the second. In general, the data for the second sampling period indicate a higher respirable mass emission rate. To what degree the respirable mass emissions were affected by sulfur trioxide concentrations is unknown. When compared to previous respirable mass data resulting from Illinois No. 6 coal firing, the integrated average data are similar within an order of magnitude range, 0.002 to 0.016 mg/m^3 . Even the emission spikes as a function of cleaning cycles were typically 0.06 mg/m^3 in April and May 1999.

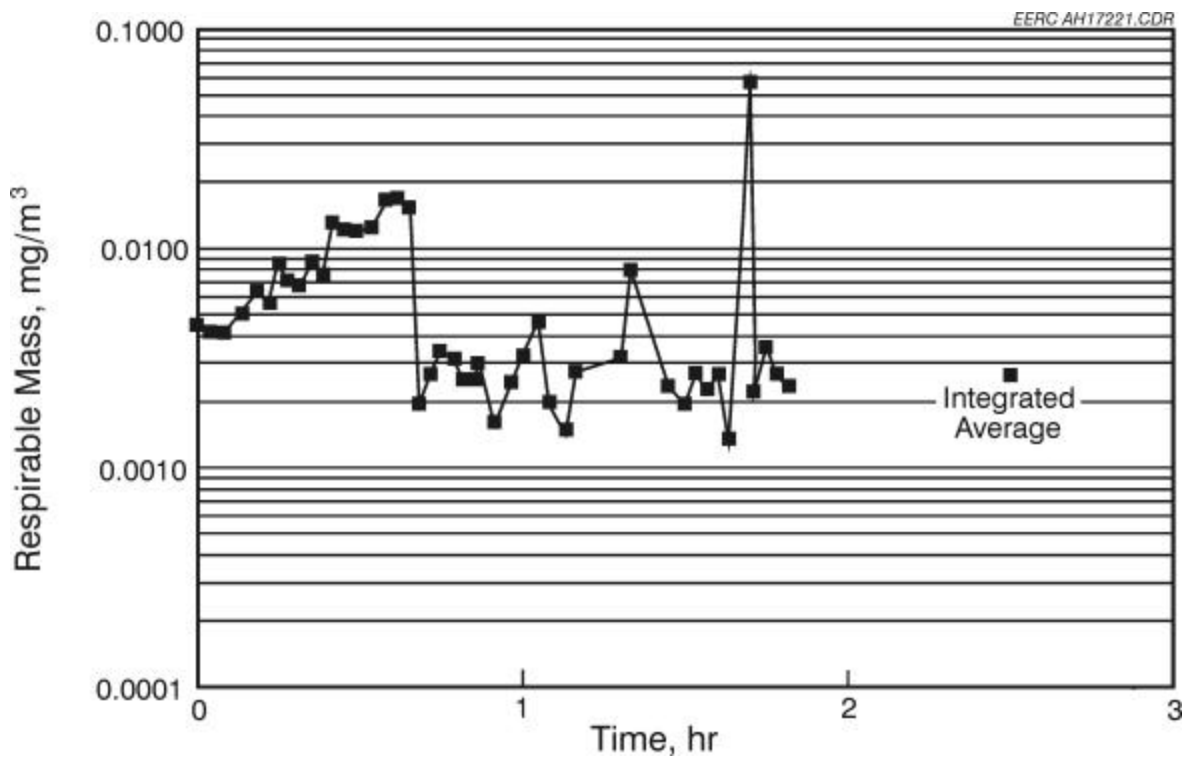
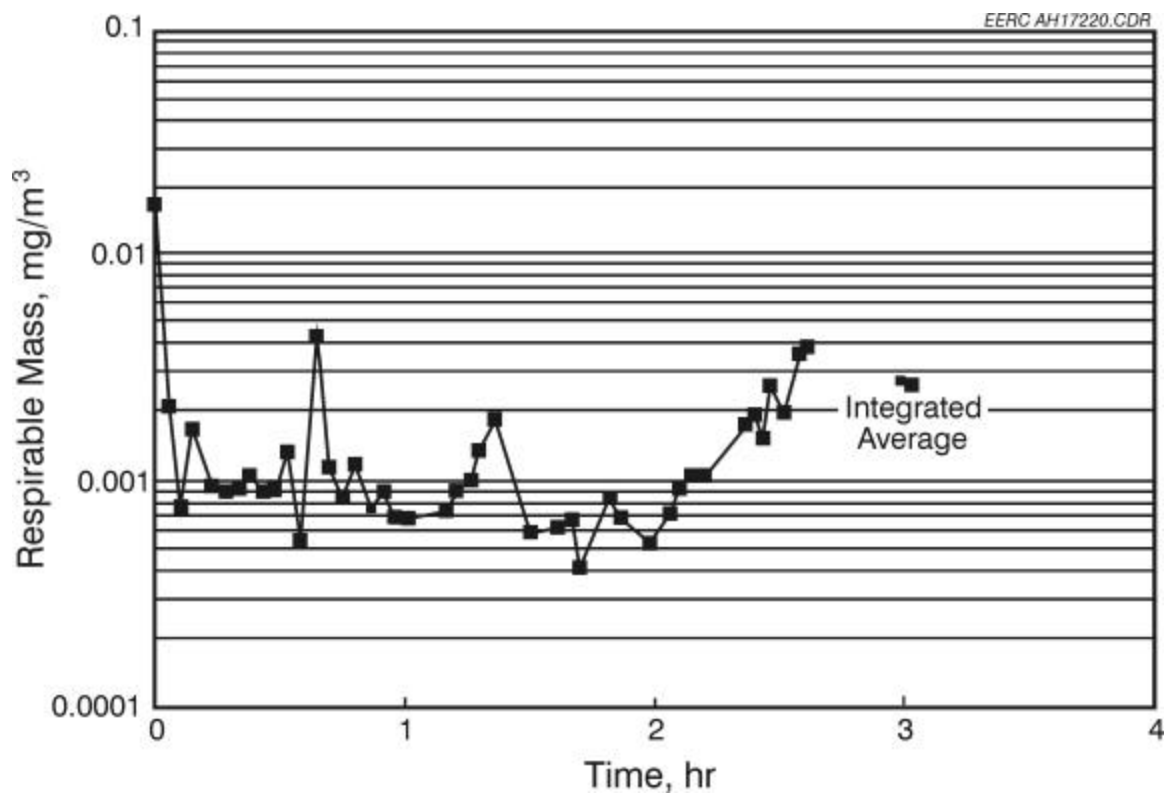


Exhibit 2-9
Respirable Mass Emissions Data for the December Test

Because of the acid condensation observed and the variability observed in particulate emissions from the pulse-jet baghouse, several bags were removed for inspection following the December test. The bags were found to be in good condition, and there was no evidence of fly ash tracking on the tube sheet. Therefore, the EERC believes that variations in flue gas sulfur trioxide concentration downstream of the baghouse were the primary contributing factor to the variable particulate emissions measured. If this conclusion is valid, particulate sampling data collected during the SFS test completed in March should be much less variable because the low sulfur content of the fuel (Cordero Rojo subbituminous coal) and the high alkali content of the fuel ash should result in essentially no sulfur trioxide in the flue gas downstream of the pulse-jet baghouse.

Particle-size analysis was completed for a composite ash sample collected from the baghouse hopper for the December test. The data show the ash to be 100 wt% <11.5 μm , 80 wt% <9 μm , and 50 wt% <5 μm for the Illinois No. 6 coal. These values indicate an ash particle size comparable to that observed when Illinois No. 6 coal was previously fired.

Multicyclone sampling data indicated a very different particle-size distribution, 70 wt% <9 μm and 50 wt% <0.8 μm for the Illinois No. 6 coal. Again, the large mass fraction observed to be <1 μm is believed to be influenced by the sulfur trioxide concentration in the flue gas. Previous multicyclone data has typically shown a similar if not larger average particle size when compared to bulk ash analyses for samples resulting from the firing of Illinois No. 6 coal.

Carbon content of the baghouse ash was measured to determine combustion efficiency. The carbon content was 0.10 wt% for the December test, somewhat lower than the 0.50 wt% carbon value observed in January and May 1999. This difference is believed to result from the improved coal pulverization previously discussed.

Pulse cleaning of the bags was accomplished on-line using a reservoir pulse-air pressure of nominally 60 psig (4.2 bar). The baghouse differential pressure cleaning set point was initially 6 in. W.C. (11 mm Hg). Once the initial dust cake was formed, the cleaning period was about 2.5 hr. The bags consistently cleaned to a differential pressure of <3 in. W.C. (<6 mm Hg). After roughly 150 hr of coal firing and overall SFS differential pressure increased, the cleaning cycle set point was reduced to 5 in. W.C. (9 mm Hg) in an attempt to mitigate system upset conditions caused by the change in overall system pressures following baghouse cleaning. This set point change resulted in a smaller swing in system differential pressure and was a beneficial change in operating protocol.

Table 2-4 shows the average flue gas composition measured during the December test. The data are based on furnace exit measurements made in the slag screen outlet. The CO concentrations in the slag screen were as high as 300 ppm and nominally 40 to 200 ppm during the December test. The high CO concentration measured in the slag screen indicates that some combustion was taking place in the slag screen. This observation may be the result of the auxiliary burner firing rate or, more likely, the firing characteristics of the Illinois No. 6 fuel in December. CO was not observed at the baghouse outlet sampling location unless the slag tap burners were operated at substoichiometric conditions, indicating that any CO observed in the slag screen was oxidized in the dilution/quench zone and CAH section.

Table 2-4
Slag Screen Flue Gas Composition for the Illinois No. 6
Coal-Fired SFS Test

| | Concentration | lb/MMBtu |
|-----------------|---------------|-----------|
| O ₂ | 3.2%–4.8% | – |
| CO ₂ | 12.6%–15.0% | – |
| CO | 40–300 ppm | – |
| NO _x | 410–580 ppm | 0.83–1.21 |
| SO ₂ | 1950–2320 ppm | 5.5–6.5 |

NO_x concentrations in the flue gas ranged from 410 to 580 ppm. Total NO_x emissions (reported as nitrogen dioxide) were determined to range from 0.83 to 1.21 lb/MMBtu. Within the range reported, NO_x emissions were stable during the December test. Also, NO_x emissions were marginally higher in December when compared to Illinois No. 6 coal-fired periods in April and May 1999. This observation is believed to result from the lower moisture content (nominally 3 wt% versus 4–5 wt%) of the fuel fired in December resulting in higher furnace flame temperatures. The auxiliary burner firing condition is also believed to have affected the NO_x concentrations and emissions; however, no specific tests have been conducted to document the effect of the auxiliary burner on NO_x emissions.

No attempt at controlling sulfur emissions was made. Calculated maximum theoretical sulfur dioxide emissions were 11.8 to 12.8 lb/hr (5.4 to 5.8 kg/hr) or 5.7 to 6.0 lb/MMBtu for the Illinois No. 6 bituminous coal. These rates are based on the main burner firing rate and the sulfur content and heating value of the fuel. The sulfur dioxide emissions, calculated on the basis of measured sulfur dioxide in the flue gas, flue gas flow rate, and the coal firing rate, resulted in values ranging from 5.5 to 6.5 lb/MMBtu. The most likely explanation for the difference in calculated sulfur dioxide emission rates, 5.7–6.0 versus 5.5–6.5 lb/MMBtu, is that the composite fuel samples that were analyzed did not adequately represent the sulfur variability documented by the flue gas analyzers.

Testing of the CAH Tube Bank

Exhibits 2-10 through 2-12 summarize CAH tube bank surface and flue gas temperatures, process air temperatures, and process air flow rate data for the December test. Exhibit 2-13 illustrates the location of thermocouples in the CAH tube bank, and Table 2-5 presents a list of thermocouple descriptions.

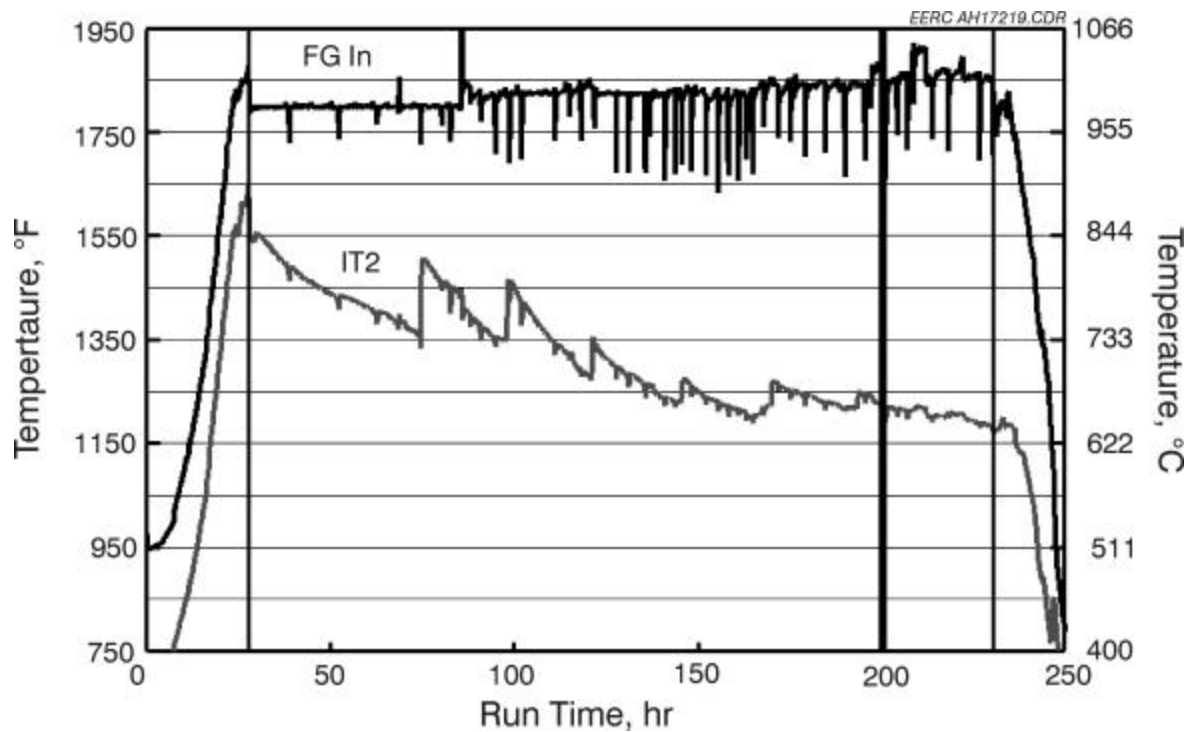


Exhibit 2-10
CAH Tube Surface and Flue Gas Temperatures Versus Run Time for the December Test, SFS-RH11-0799

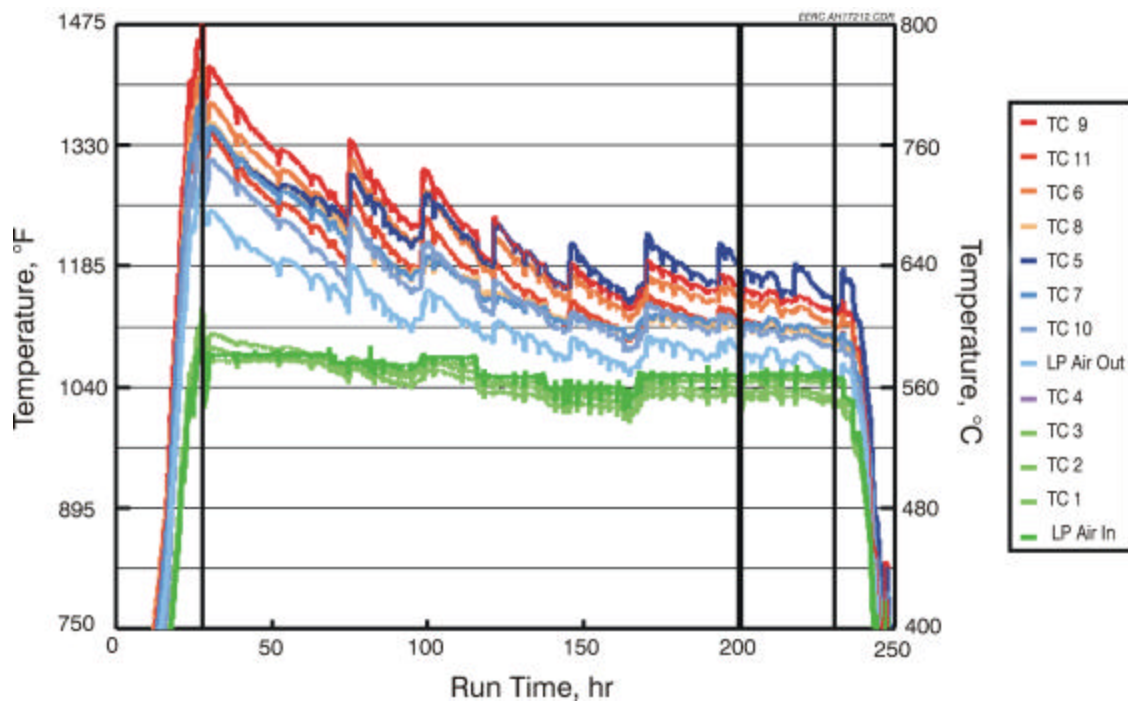


Exhibit 2-11
CAH Process Air Temperatures Versus Run Time for the December Test, SFS-RH11-0799

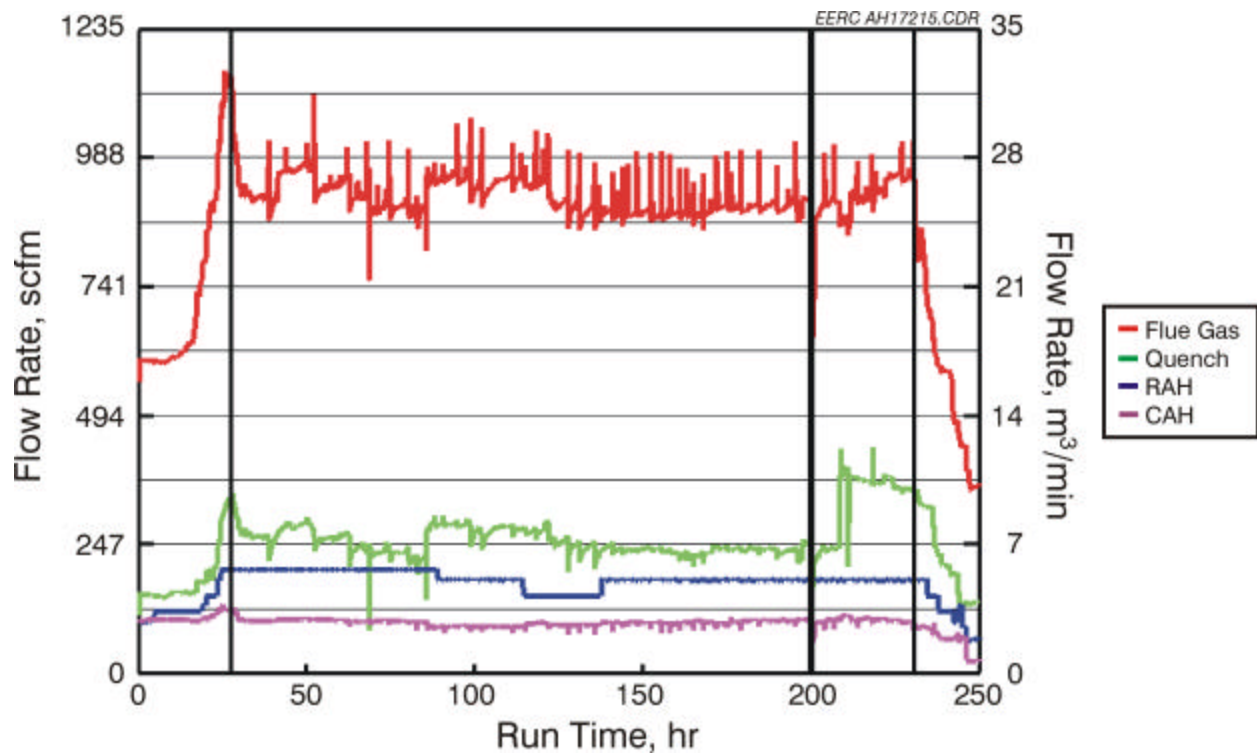


Exhibit 2-12

CAH Process Air, RAH Process Air, Quench Gas, and Flue Gas Flow Rates Versus Run Time for the December Test, SFS-RH11-0799

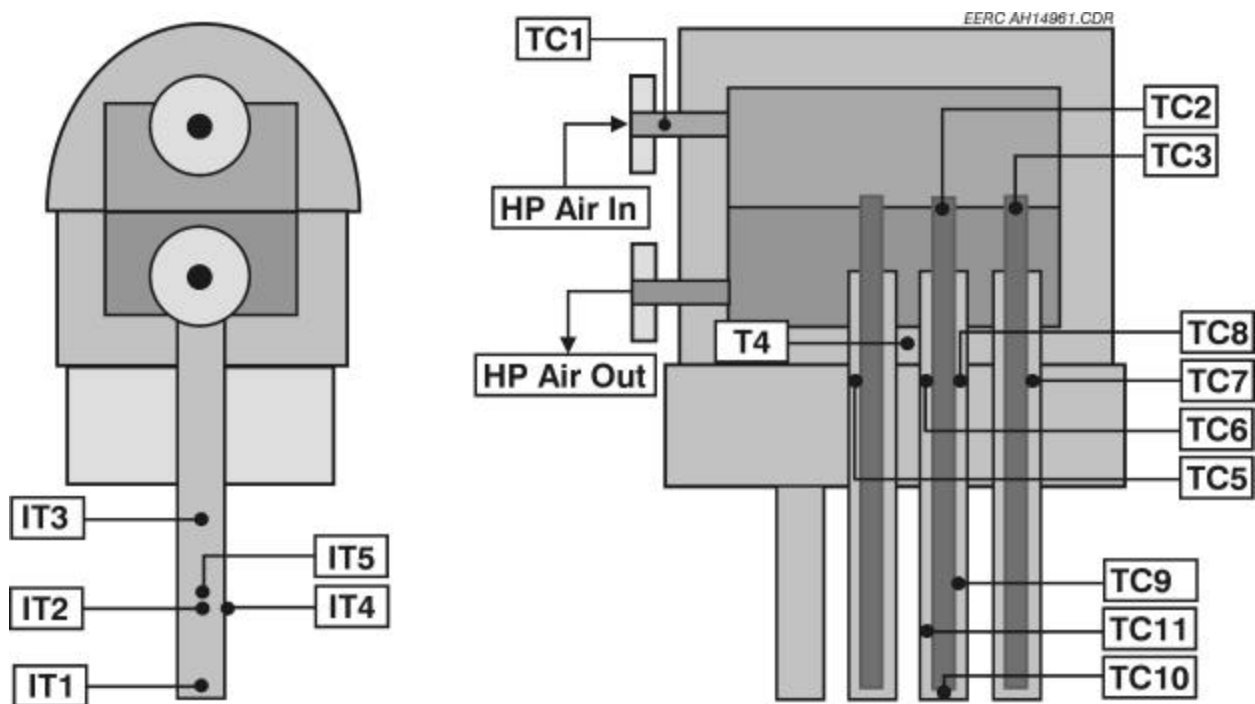


Exhibit 2-13

Thermocouple Locations in the CAH Tube Bank

Prior to an August 1998 test, all of the CAH thermocouples were replaced or repaired in conjunction with the installation of fins on the air-cooled tubes. However, one tube surface thermocouple (CAHIT3) was damaged when the tube bank was installed in the flue gas duct. One additional CAH thermocouple failed during both the August and December 1998 tests, and a fourth thermocouple failed at the beginning of a January 1999 test. Therefore, during the December test, only one of the five surface thermocouples was functioning properly. There are no plans to replace these thermocouples at this time because of the time and expense that would be required.

On the basis of a single thermocouple measurement, the clean tube surface temperatures were nominally 1540°F (838°C), with the surface temperature decreasing to 1190°F (644°C) as ash deposits developed and adjustments were made to the process air flow rate. Attempts to sootblow the CAH tube bank are evident in the data as step increases in surface temperature. The general decline in measured surface temperature over the initial 120 hr of coal firing demonstrate that the sootblowing approach used in December was not effective. However, the surface temperature data during the last 50+ hr of coal firing indicate that an equilibrium may have been reached and that continued sootblowing would have maintained surface temperatures in the range of 1090° to 1280°F (644° to 694°C).

Because the approach to sootblowing used during the December SFS test was not entirely effective, more frequent sootblowing was used during the March SFS test. The components of the sootblowing system remained the same as did the media (nitrogen gas) and media pressure (200 psig/13.8 bar) and flow rate (188 scfm/5.3 m³/min). The approach simply involved the manual insertion and removal of a probe through an access port to the tube bank. This approach permits sootblowing between two rows of tubes. The duration of an actual sootblowing event did not exceed 15 sec. During the March SFS test, the EERC began sootblowing after 8 hr of coal firing and then repeated sootblowing every 8 hr for the duration of the test. The results of the March CAH sootblowing effort are not available for discussion at this time.

Table 2-5
Description of CAH Thermocouple Locations¹

| Category | No. | Label | Description |
|---------------|-----|---------|---|
| Air Inlet | 1 | CAHTC1 | Bulk flow entering the inlet header |
| | 2 | CAHTC2 | Air entering center tube |
| | 3 | CAHTC3 | Air entering most downstream tube |
| Air Outlet | 4 | CAHTC6 | Air leaving center tube |
| | 5 | CAHTC7 | Air leaving most downstream tube |
| | 6 | CAHTC5 | Air leaving most upstream tube |
| | 7 | CAHTC8 | Air leaving side tube |
| Air in Active | 8 | CAHTC10 | Bottom of center tube |
| | 9 | CAHTC11 | 4 in. up outside annulus, center tube |
| | 10 | CAHTC9 | 8 in. up outside annulus, center tube |
| Tube Surface | 11 | CAHIT1 | 1 in. up center tube, facing upstream (failed) |
| | 12 | CAHIT2 | 5 in. up center tube, facing upstream |
| | 13 | CAHIT3 | 8 in. up center tube, facing upstream (failed) |
| | 14 | CAHIT4 | 5 in. up center tube, facing to side (failed) |
| | 15 | CAHIT5 | 5 in. up center tube, facing downstream (failed) |
| Header Shell | 16 | CAHTC4 | Next to shell on outside, between return air pipes (failed) |

¹ Thermocouple locations are illustrated in Exhibit 2-13.

While natural gas was fired and the tubes were clean, heat recovery from the CAH tube bank was roughly 40,000 Btu/hr (42,200 kJ/hr) in December. The process air flow rate was 120 scfm (3.4 m³/min). The inlet process air temperature was 1090°F (588°C), outlet process air was 1245°F (674°C), and flue gas was 1800°F (982°C) entering the CAH tube bank. Exhibit 2-14 presents heat recovery in the CAH as a function of run time.

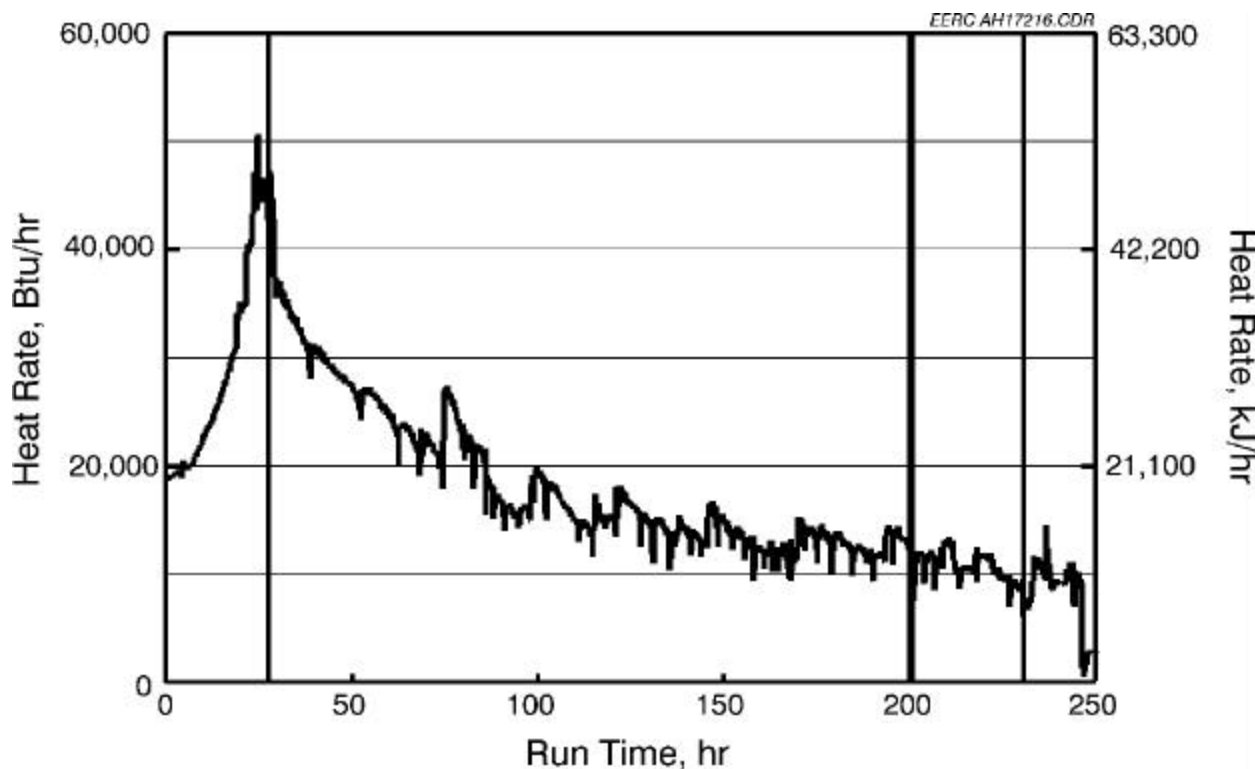


Exhibit 2-14

CAH Heat Recovery Versus Run Time for the December Test, SFS-RH11-0799

When coal firing began, surface temperatures initially decreased at a rate of nominally 4.5°F/hr (2.5°C/hr) over nearly 25 hr as ash deposits developed on the surface of the tubes. After 45 hr of coal firing, an attempt was made to sootblow the CAH tube bank. As a result, the tube surface temperature increased from 1355°F (735°C) to 1505°F (819°C), and the heat recovery rate increased from 20,000 Btu/hr (21,100 kJ/hr) to 27,300 Btu/hr (28,802 kJ/hr). After an additional 24 hr of coal firing, CAH sootblowing was repeated. A surface temperature increase was again observed, 1345°F (730°C) to 1460°F (794°C). However, the heat recovery rate increase, 16,200 Btu/hr (17,091 kJ/hr) to 19,400 Btu/hr (20,467 kJ/hr) was lower because it was necessary to reduce the process air flow rate (103 to 90 scfm/2.9 to 2.5 m³/min) in order to maintain process air temperature in support of RAH operation. Based on the data in Exhibit 2-14, it appears that sootblowing should have begun after 8–12 hr of coal firing and repeated every 8–12 hr in order to maintain a heat recovery rate in the CAH tube bank of >30,000 Btu/hr (>31,650 kJ/hr).

The approach to sootblowing in December was not effective, and no attempt had been made to sootblow the CAH tubes prior to the installation of fins. Therefore, conclusions cannot be drawn concerning the potential advantages of the fins when routine sootblowing is effectively used to maintain desired CAH heat recovery. However, previous data support the conclusion that the addition of the fins to the air-cooled tubes improves heat recovery during the coal-fired test periods. The fins appear to reduce the rate of heat-transfer degradation as ash deposits develop and help to maintain a higher heat-transfer rate once the deposits have formed. However, no improvement in heat recovery was observed during the initial natural gas-fired periods with clean tube surfaces.

Because of the attempts to sootblow the CAH tube bank during the December test and previous characterization of CAH ash deposits resulting from Illinois No. 6 coal-fired tests, CAH ash deposits were not collected for characterization following the test. The deposits that formed were limited to the leading and trailing edges of the tubes. Exhibit 2-15 presents a photograph of ash deposits on the surface of the tubes following the December test. The photograph shows three of the five uncooled tubes as well as two of the seven air-cooled finned tubes. Substantial leading- and trailing-edge deposits are visible. However, CAH tube bank plugging was not a problem. No deposits were observed bridging the flue gas path between the tubes.



Exhibit 2-15
Photograph of Ash Deposits on the CAH tubes Following the December Test
Firing Illinois No. 6 Bituminous Coal

Deposit strength is a function of ash chemistry, particle size, and temperature history. The relative strength of the deposits is indicated by the fact that the deposits remained intact when the tube bank was removed from the duct. This observation is consistent with results from previous tests firing Illinois No. 6 bituminous coal. The total weight of the deposits collected from the CAH tubes and duct was 165 lb (74.9 kg). The total weight of the deposits collected from the CAH tubes was 24 lb (11 kg). On a mass per unit time basis, the ash deposition rate on the CAH tubes would be 0.12 lb/hr (54.5 g/hr) of coal firing. Incorporating the surface area of the tube bank (6.28 ft² or 0.58 m²) results in a value of 0.019 lb/hr-ft² (93.97 g/hr-m²). On a coal-firing-rate basis, the CAH ash deposition rate would be 0.06 lb/MMBtu (25.9 g/10⁶ kJ). These values are marginally higher than those reported for the Illinois No. 6 coal fired in May 1999 and at least 33% higher than those observed in September 1998. The higher ash deposition rate observed in December 1999 is believed to result from a lower slag screen

efficiency. Slag screen efficiency was lower because there were only nine tubes present versus 18 tubes typically used during previous tests firing Illinois No. 6 coal.

Testing of the RAH Panel

Initial shakedown and testing of the RAH panel took place in December 1997. Testing of the RAH panel continued this past quarter with completion of an SFS test in March 2000. However, data from the March test are not available for discussion at this time. Therefore, the balance of the RAH discussion will focus on the December 1999 test data following RAH tile replacement in early December. The primary purpose of the December (SFS-RH11-0799) test was to evaluate the ability of the new Kyocera tile to withstand the slag attack and thermal cycling conditions in the slagging furnace. In addition, RAH panel performance was evaluated relative to heat transfer, tile and tube temperatures, and process air temperatures and flow rates. Generally, the performance of the RAH panel in December was nominal, with no significant process or material problems observed.

The ceramic tiles were removed from the RAH panel in November 1999 in preparation for the installation of new tiles in December. The RAH panel ceramic tiles were thoroughly inspected upon installation. Exhibit 2-16 illustrates the cracks found in the tiles/bricks, and Exhibit 2-17 is a photograph of the furnace interior after the tiles were installed. The three new fusion-cast alumina Monofrax M tiles (small upper tile, large lower tile, and small lower tile) had minor cracks. In addition, the small lower tile had one significant crack that extended from the top to the bottom edge. None of these cracks is visible in the photograph.

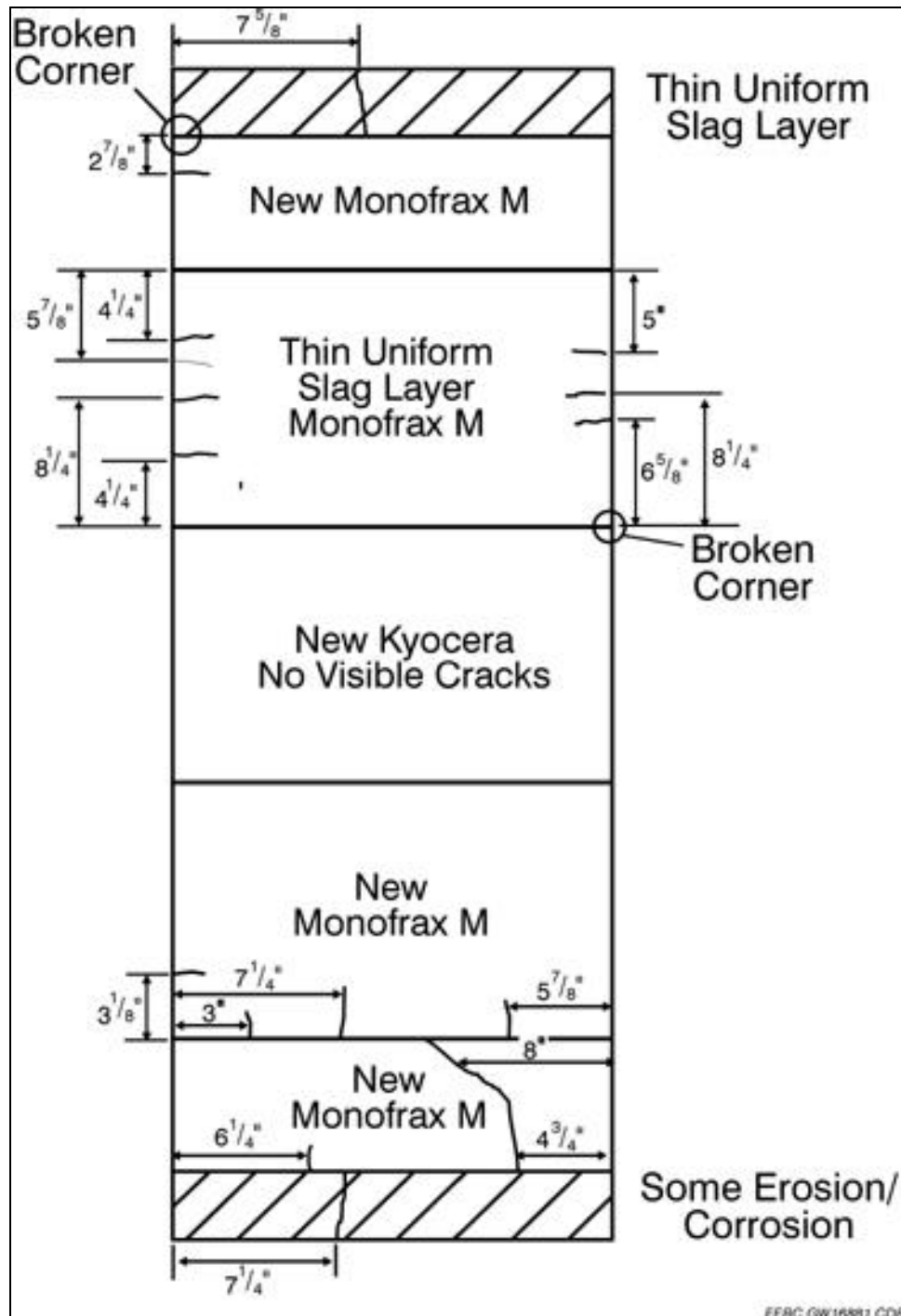


Exhibit 2-16

Illustration of Cracks Found in the New and Used Ceramic Tiles/Bricks Installed in the RAH Panel Prior to the December Test, SFS-RH11-0799

Only one new sintered chromia–alumina Kyocera tile was installed because a second tile had four broken corners as well as a large number of small cracks extending from each edge. The damage to the second Kyocera tile occurred as a function of curing and machining prior to shipment to the EERC. The new Kyocera tile was installed in the center tile position and did not have any visible cracks. However,

the upper right corner of the Kyocera tile was broken as a result of some machining that was performed at the EERC prior to its installation. Because only one large new Monofrax M tile was available, it was necessary to reuse one of the Monofrax M tiles originally installed in January 1999 as a replacement for the second Kyocera tile. This large tile had been in the lower position on the panel and is now in the upper position, as seen in the Exhibit 2-17 photograph. Five cracks were evident in this tile prior to the December test, four extending from the left edge and three extending from the right edge. The top and bottom support bricks were reused, with each having one vertical crack extending through the face.



Exhibit 2-17
Photograph of the Ceramic Tiles Installed on the RAH Panel Prior to the December Test

The RAH panel ceramic tiles were thoroughly inspected following the December test period. Exhibit 2-18 presents a photograph of the RAH panel from inside of the furnace after the December test. Although the condition of the RAH ceramic tiles is not clearly depicted in this photograph, the Kyocera tile is evident from its color and surface characteristics. The Kyocera tile is lighter in color when compared to the Monofrax M tiles and the surface appears smooth. Although the photograph indicates erosion/corrosion of the Kyocera and Monofrax M tiles, the degree of erosion/corrosion is more pronounced on the Monofrax M tiles. Quantitative measurement of this difference will only be possible when the tiles have been removed from the RAH panel for characterization.



Exhibit 2-18
Photograph of the RAH Panel Inside of the Slagging Furnace Following the December Test

A residual slag layer on the surface of the new Monofrax M tiles following coal firing in December 1999 caused the surface of the tiles to darken, white to a brown/black. For the Kyocera tile, the color change was from a reddish hue to a gray. The color change in the Monofrax M tiles is consistent with previous observations, and no additional color change is anticipated based on past experience. Further color changes to the Kyocera tile are not expected. Although not obvious in the photos, the slag layer on the tiles is thin and appears to be uniform, with no evidence of any extensive slag buildup. While slag is present in the seams between the tiles, there is no evidence of any fusion between adjacent tiles. Therefore, the 4-hr period of natural gas firing at full load prior to SFS cooldown appears to be adequate to prevent buildup of excess slag on the surface of the tiles or in the seams between tiles. Also, any quantity of slag present in the seams between tiles appears to crack as a result of cooldown and tile movement.

Exhibit 2-19 illustrates the visible cracks found in the RAH tiles following the December test. Overall, the condition of the tiles was degraded during the test. The large upper tile has been exposed to furnace conditions for the greatest length of time and, as a result, shows the greatest degree of erosion/corrosion when the three large tiles are compared. Following completion of the December test, only the small upper and lower tiles were observed to be free of visible cracks. However, at least one crack was evident in each of these tiles prior to the December test, demonstrating the potential for

hairline cracks to be covered with slag. A similar observation was made for the two large Monofrax M tiles. Seven cracks were evident in the large upper tile prior to the December test, with only three visible following the test. Four cracks were evident in the large lower tile prior to the December test with a single new crack visible following the test.

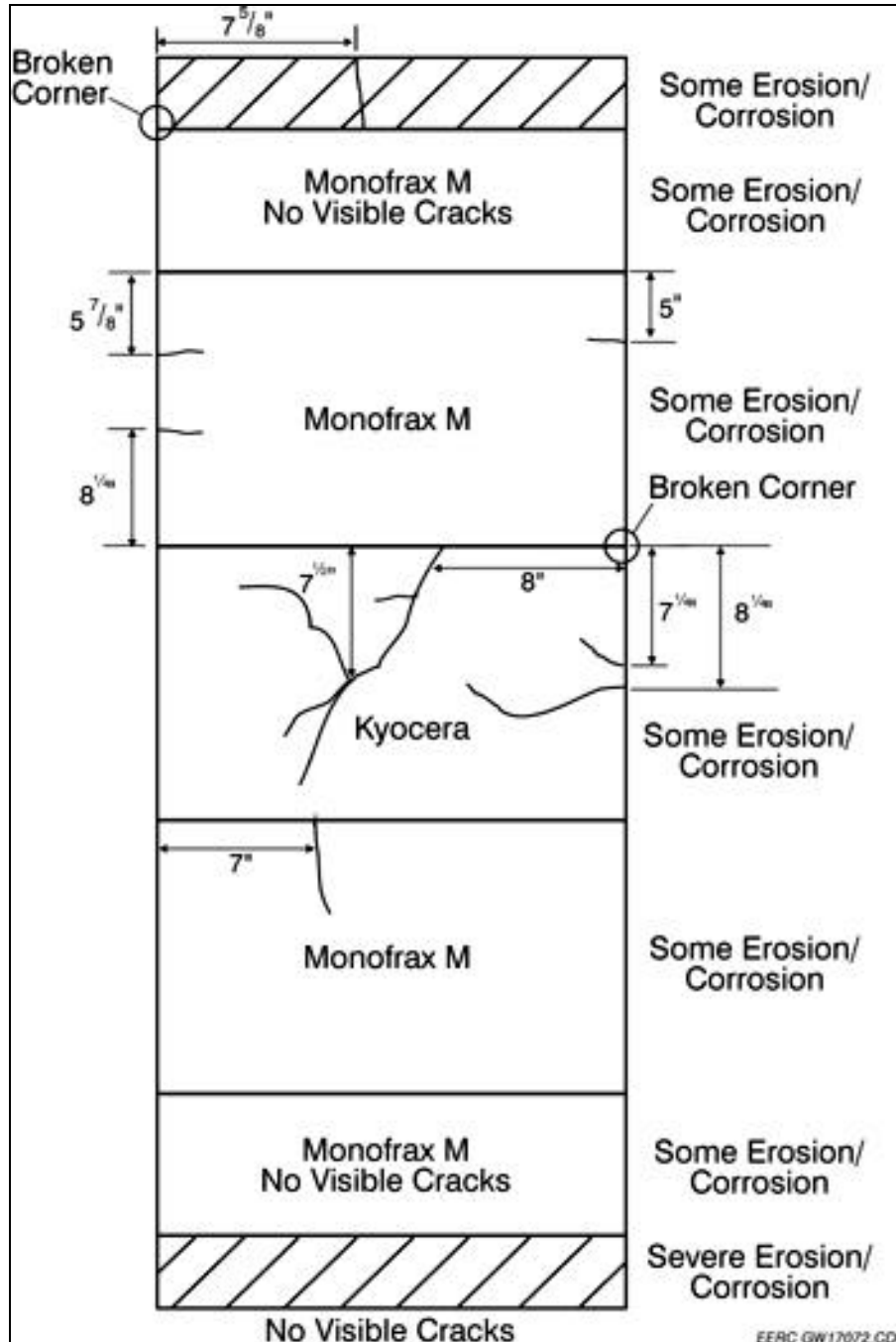


Exhibit 2-19
Illustration of Cracks Found in the Ceramic Tiles/Bricks of the RAH Panel
Following the December Test

There were no visible cracks in the Kyocera tile prior to the December test. Following the test, two cracks were evident originating from the right edge and one from the top edge. The two cracks originating from the right edge are hairline cracks not visible in photographs and similar to those observed in the Monofrax M tiles. The crack originating from the top edge of the Kyocera tile is visible in the Exhibit 2-18 photograph as it extends from the top edge down and left. The photograph in Exhibit 2-20 shows the crack more clearly as well as one of the three hairline cracks illustrated in Exhibit 2-18 that branch from the original crack. One hairline crack branches up and left while two extend down and left. This type of radial cracking was observed previously in one Monofrax M tile. Although the cracks observed in the Kyocera tile are not believed to indicate impending tile failure, the more open area of the crack was filled/covered with an alumina cement prior to the March test. The degree of slag erosion/corrosion experienced by the Kyocera tile is also evident in the Exhibit 2-20 photograph. The most significant area of erosion/corrosion is observed at the top edge where slag dripped from the tile above. Slag channels that developed on the surface of the Kyocera tile are also evident in the photograph. Compared to the Monofrax M tiles, there were fewer corrosion channels, and they were not nearly as deep. In addition, the slag did not appear to penetrate into the Kyocera tile nearly as much as into the Monofrax M tile. An interesting feature of the slag corrosion of the Kyocera tile is the formation of spots of frozen slag near the bottoms of many of the slag corrosion rivulets. The spots of frozen slag are reddish in color and highly crystalline. It is believed that the spots formed as the slag dissolved enough of the chromium from the tile to increase the melting point of the slag to the point that crystals formed and precipitated from the slag.



Exhibit 2-20
Photograph of the Large Kyocera Tile Following the December Test

The small lower tile continues to show the greatest degree of erosion/corrosion. This is believed to result from the combination of its higher surface temperature and the greater quantity of slag flowing over its surface during SFS tests relative to the other tiles. The surface temperature of the small lower tile, although not measured, is believed to be higher than the three larger tiles, because the backside of

this tile is insulated and is not directly cooled by the heat-transfer surfaces. The greatest quantity of slag also flows over this tile because of its location below the other tiles. Exhibit 2-21 presents a photograph of the small lower tile.



Exhibit 2-21

Photograph of the RAH Small Lower Tile Following the December Test

Heatup/cooldown cycles are believed to be the primary cause of RAH panel ceramic tile/brick crack propagation for both the Monofrax M and Kyocera tiles. Slag contributes to erosion/corrosion of surfaces and imparts stresses on the ceramic tiles as it finds its way into seams between tiles. Photographs in Exhibits 2-18, 2-20, and 2-21 illustrate the small quantity of slag found in the seams between the tiles.

Exhibits 2-22 through 2-24 summarize the RAH ceramic tile temperatures, tube surface temperatures, and process air temperatures for the December test (SFS-RH11-0799). The process air flow rate data for the RAH panel were summarized in Exhibit 2-12. Exhibit 2-25 illustrates the location of thermocouples in the RAH panel, and Table 2-6 describes the RAH thermocouples. The indicated ceramic tile surface temperatures (cavity-side) ranged from nominally 1605° to 1955°F (874° to 1069°C), based on measurements made at the center of each of the three large tiles once the SFS had stabilized thermally (Run Hours 35 through 230). Unfortunately, thermocouple T22 failed at Run Hour 72. Thermocouple T23 was not used when the Kyocera tile was installed. Therefore, a furnace-side tile surface temperature measurement is not available. UTRC and EERC elected not to install thermocouple T23 to avoid potential damage to the Kyocera tile. All tile surface temperatures (cavity-side) during the December test were lower than the temperatures observed during the RAH Kentucky coal-fired test in September. This difference would appear to be the result of the higher furnace firing rate (nominally 10%) and furnace gas temperatures (55° to 85°F/31° to 47°C) in September. However, comparing December cavity-side tile temperatures

with those observed in May (firing Illinois No. 6 bituminous coal and maintaining comparable furnace temperatures) shows an even more significant temperature difference (310° to 445°F/172° to 247°C). This temperature difference was measured even though RAH tube temperatures and heat recovery in December and May were similar. Therefore, it is believed that the tile surface temperatures measured in December were not valid. One possible explanation would be that the thermocouples became detached from the tile surfaces and were simply measuring a cavity temperature. Further evaluation of the tile surface temperatures will occur as a result of the March 2000 test.

Table 2-6
Description of RAH Panel Thermocouple Locations¹

| Category | No. | Label | Description |
|----------------------------------|-----|-----------|---|
| Air Inlet | 1 | HP Air In | Provided by the EERC, in pipe before inlet |
| | 2 | RAHT11 | Air entering RAH through center tube |
| Air Outlet | 3 | RAHT18 | Air leaving left (south) tube |
| | 4 | RAHT9 | Air leaving middle tube |
| | 5 | RAHT12 | Air leaving right (north) tube |
| MA Tube Surface | 6 | RAHT1 | Top of middle tube facing cold side |
| | 7 | RAHT2 | Middle of middle tube facing other tube |
| | 8 | RAHT3 | Top of middle tube facing toward furnace |
| | 9 | RAHT4 | Middle of middle tube facing cold side |
| | 10 | RAHT5 | Middle of middle tube facing toward furnace |
| | 11 | RAHT6 | Bottom of middle tube facing cold side |
| | 12 | RAHT7 | Removed |
| | 13 | RAHT8 | Removed |
| | 14 | RAHT10 | Bottom of the middle tube facing toward |
| | 15 | RAHT13 | Removed |
| | 16 | RAHT14 | Top of north tube facing toward furnace |
| | 17 | RAHT15 | Bottom of north tube facing toward furnace |
| | 18 | RAHT16 | Removed |
| | 19 | RAHT17 | Bottom of north tube facing toward side wall |
| | 20 | RAHT28 | Top of south tube facing toward furnace |
| | 21 | RAHT29 | Bottom of south tube facing toward furnace |
| Inner Surface of Monofrax bricks | 22 | RAHT19 | Top tile, center |
| | 23 | RAHT20 | Removed |
| | 24 | RAHT21 | Removed |
| | 25 | RAHT22 | Middle tile, center (failed in December 1999) |
| | 26 | RAHT23 | Middle tile, (removed December 1999) |
| | 27 | RAHT24 | Middle tile, left side rail |
| | 28 | RAHT27 | Removed |
| | 29 | RAHT25 | Lower tile, center |
| | 30 | RAHT26 | Removed |

¹ Thermocouple locations are illustrated in Exhibit 2-25.

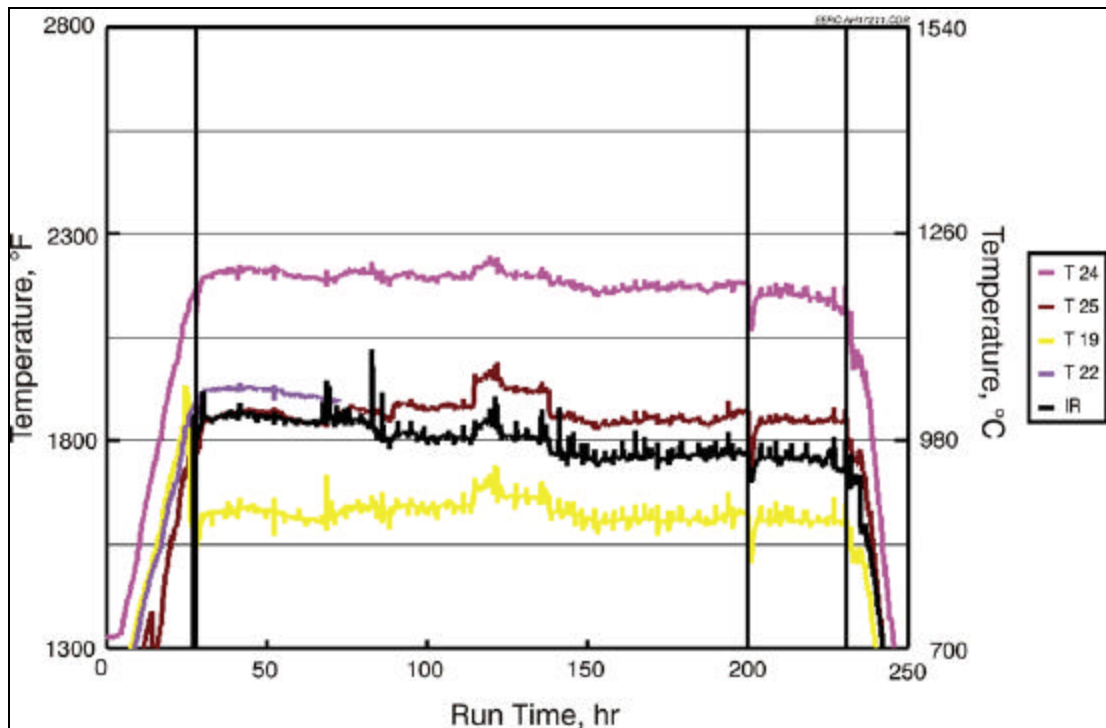


Exhibit 2-22
RAH Ceramic Tile Temperatures Versus Run Time for the December Test,
SFS-RH11-0799

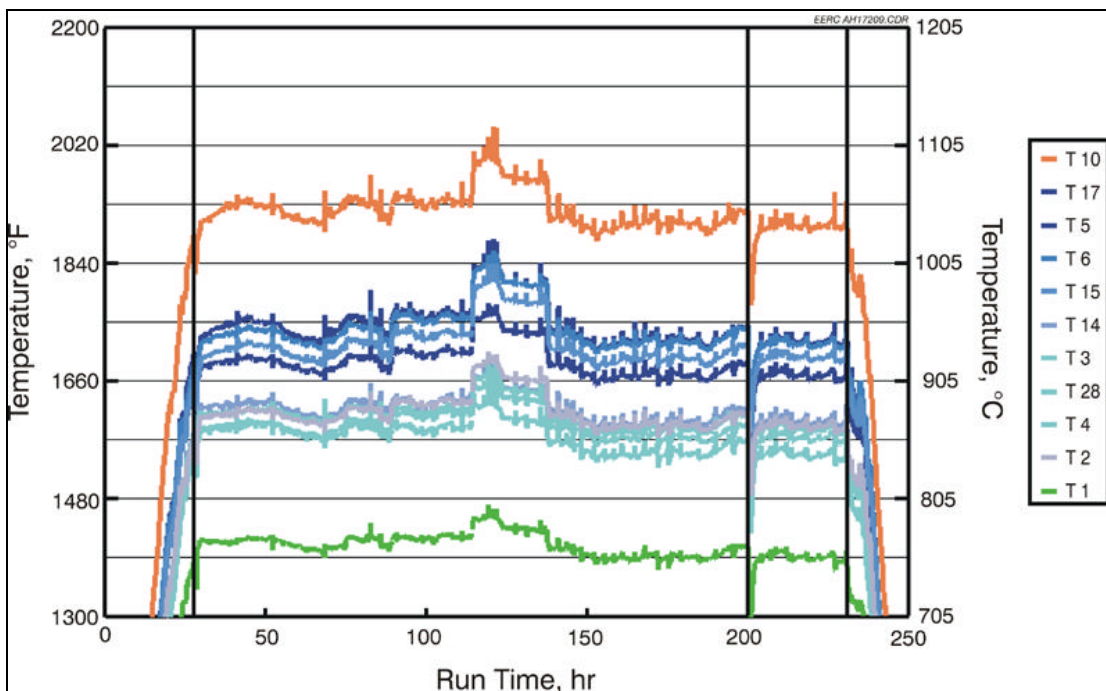


Exhibit 2-23
RAH Tube Surface Temperatures Versus Run Time for the December Test,
SFS-RH11-0799

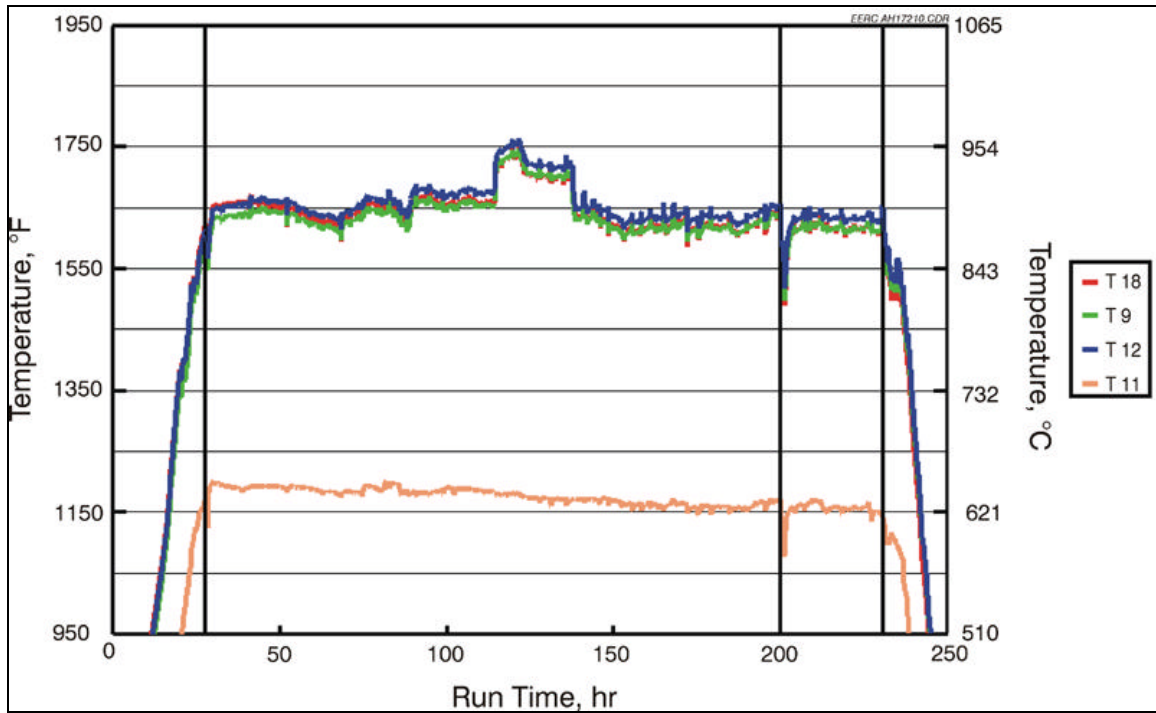


Exhibit 2-24
RAH Process Air Temperatures Versus Run Time for the December Test,
SFS-RH11-0799

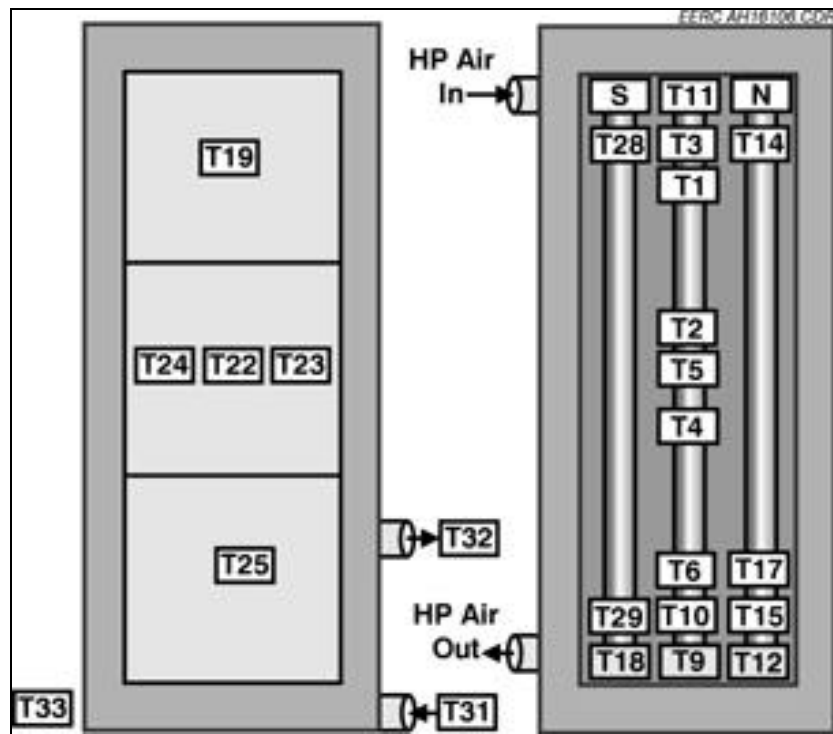


Exhibit 2-25
Thermocouple Locations in the RAH Panel

RAH process air flow rates during the December test were controlled at 150, 180, and 200 scfm (4.2, 5.1, and 5.7 m³/min), with most of the operational time split between 180 and 200 scfm (5.1 and 5.7 m³/min). Changes in process air flow rates had a definite effect on indicated tile surface temperatures. As flow rates were reduced, tile surface temperature increased. Subsequently, when process air flow rates were increased, tile surface temperatures decreased. This effect is evident for flow rate changes at Run Hours 89, 114, and 137.

RAH tube surface temperatures ranged from nominally 1390° to 2045°F (755° to 1119°C). The low end of the temperature range represents the back side of the tube surfaces near the process air inlet, with the high end of the temperature range representing the front side of the tube surfaces near the process air outlet. Changes in process air flow rates had noticeable effects on all tube surface temperatures. Tube surface temperature step changes were most noticeable for surface temperature measurements near the process air exit and on the front side of the tubes. Tube surface temperatures in December were comparable to those for all previous bituminous coal-fired tests.

Process air inlet temperatures ranged from 1155° to 1200°F (624° to 649°C) during the coal-fired operational period. Outlet process air temperatures ranged from nominally 1605° to 1755°F (874° to 958°C). The effect of process air flow rate can be seen in the process air outlet temperature data. As process air flow rate decreases, exit temperature increases, as expected. These flow rate changes are noted at Run Hours 89, 114, and 137.

Heat recovery data from the RAH panel are presented in Exhibit 2-26 for the December test. At process air flow rates of 150, 180, and 200 scfm (4.2, 5.1, and 5.7 m³/min), the heat recovered from the RAH panel was 101,430 to 106,700 Btu/hr (107,009 to 112,568 kJ/hr), 101,790 to 111,160 Btu/hr (107,388 to 117,274 kJ/hr), and 111,160 to 117,860 Btu/hr (117,274 to 124,342 kJ/hr), respectively. The heat recovery ranges are a function of minor adjustments to the coal feed rate and combustion air flow rates. The main burner firing rate was nominally 2.0 MMBtu/hr (2.1×10^6 kJ/hr).

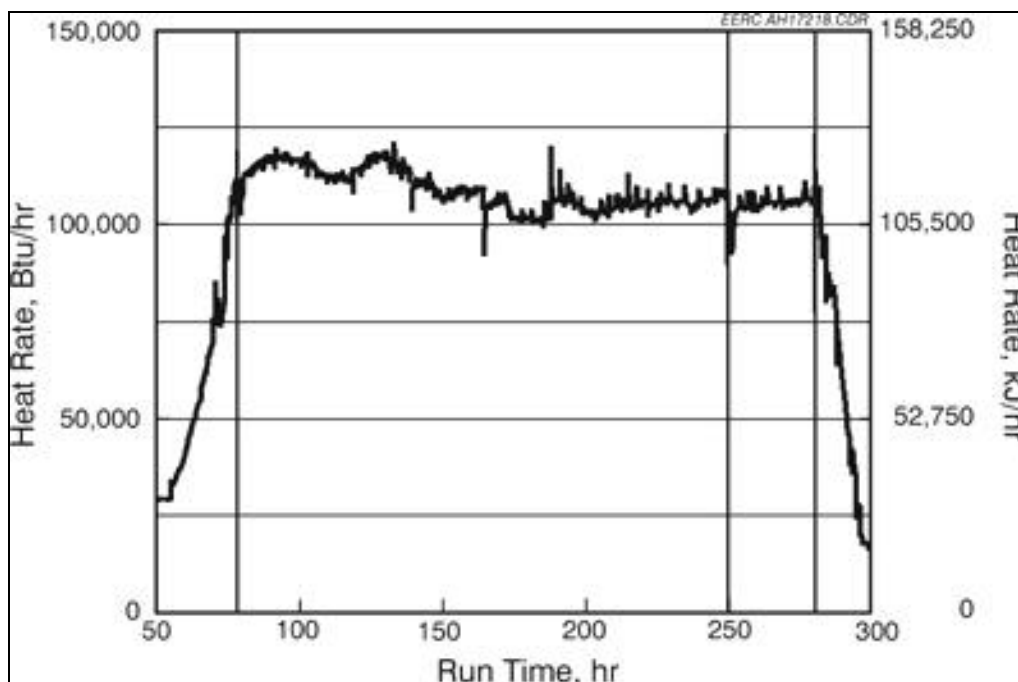


Exhibit 2-26

RAH Heat Recovery Versus Run Time for the December Test, SFS-RH11-0799

Exhibit 2-27 summarizes RAH heat recovery data at process air flow rates of 180 and 200 scfm (5.1 and 5.7 m³/min) for bituminous coal-fired tests completed in 1998 through December 1999. A comparison of the RAH panel data for the December (RH11) Illinois No. 6 bituminous coal-fired test and the May (RH9) test firing a similar fuel shows no real change in the heat recovery rate. A comparison of the heat recovery rate data for December (RH11) and September (RH10) indicate that the RAH panel heat recovery in September was higher. The reason for the higher RAH heat recovery in September was the higher average coal firing rate (10%) and resulting furnace gas temperatures (55°–85°F/31°–47°C). However, data generated in December (RH11) and January 1999 (RH6) show that the January (RH6) RAH heat recovery rate was higher (16%–17%) than the rate observed in December (RH11), even though furnace gas temperatures were similar. Therefore, coal-firing rate and furnace gas temperatures are not the only factors influencing heat transfer to the RAH panel.

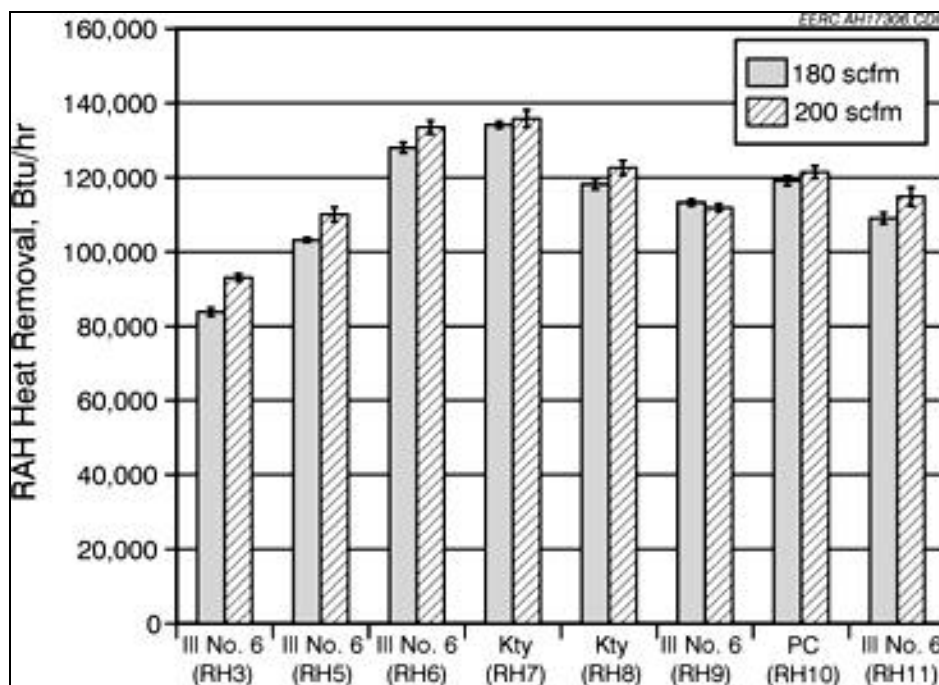


Exhibit 2-27
RAH Heat Recovery for Bituminous Coal-Fired Tests
Completed in 1998 and 1999

A comparison of the RAH panel data for the May and January 1999 tests firing Illinois No. 6 bituminous coal shows that the heat recovery rate in May was lower by 13% to 20%. However, the May heat recovery rates are comparable to those for the Illinois No. 6 bituminous coal-fired test in August 1998, where heat recovery rates in the RAH panel were <120,000 Btu/hr (<126,600 kJ/hr) for a process air flow rate of 180 scfm (5.1 m³/min). A similar comparison to data generated in February 1998 shows that the RAH heat recovery rate in May 1999 was 25% higher at comparable SFS operating conditions.

The reasons for the variations in heat recovery rate are twofold. First, for tests up to and including the August 1998 tests, a small RAH was also present in the furnace. This removed heat from the furnace and reduced the heat recovery rate by the RAH. After the August 1998 test, the small RAH was removed from the system. Therefore, direct comparisons of RAH heat recovery are only valid for tests completed over the past 15 months (RH6, RH7, RH8, RH9, RH10, and RH11). A second reason for heat recovery variability in the RAH can be seen in comparisons of RH6 and RH9 (firing Illinois No. 6 coal), and RH7 and RH8 (firing eastern Kentucky coal). In both cases, heat recovery by the RAH was lower for the second test for each coal type. These data indicate that the heat recovery rate for the RAH panel is decreasing with each week of operation.

The reason for this reduction in heat recovery with time is not well understood, but EERC personnel believe that several factors are influencing the reduction. One possibility is a potential change in heat flux to the RAH ceramic tiles resulting in a decrease in the heat transfer to the radiation cavity. The flame-side surface of the RAH ceramic tiles did darken as a result of slag coating and absorption during the January 1999 test. However, it is not clear what the effect would be on radiant heat absorption or

emission or thermal conductivity. Also, no additional color changes were noted following subsequent test periods. Another possibility is that the changing heat flow may be related to ceramic tile deterioration with each week of coal-fired furnace operation as a result of slag erosion/corrosion. Erosion/corrosion of the ceramic tiles may be affecting their heat-transfer properties. However, if thinning of the RAH ceramic tiles were the controlling factor, RAH heat recovery in December should have been higher than that observed in May.

Another potential contributing factor to the decreasing heat flow may be the high-density furnace refractory color change observed with each week of operation. As the high-density refractory has darkened with each week of operation, it is possible that the reflectivity or emissivity characteristics of the furnace liner have changed, resulting in a decrease in radiation to the RAH panel. A combination of effects due to changes in tile and high-density refractory characteristics may be a reasonable explanation. That combination of factors would explain a lower RAH heat recovery rate in December (RH11, new tiles and aged high-density refractory) when compared to January (RH6, new tiles and high-density refractory), yet a comparable RAH heat recovery rate when compared to May (RH9, aged tiles and high-density refractory).

Table 2-7 summarizes operating time for the SFS, CAH tube bank, and RAH panel. Through February 2000, the RAH panel has been exposed to a range of furnace-firing conditions for a total of 2340 hr. Natural gas firing represents 1238 hr (including heatup, cooldown, and refractory curing), and coal/lignite firing represents 1102 hr. In addition, the RAH panel has been exposed to fifteen heating and cooling cycles. The RAH ceramic tiles that were installed in January 1999 and removed in December 1999 were exposed to six heating and cooling cycles and 988 hr of slagging furnace operation: 473 hr of natural gas firing (including heatup and cooldown) and 515 hr of coal firing. With the exception of the one Monofrax M tile that was reused, the RAH ceramic tiles that were installed in December 1999 have been exposed to two heating and cooling cycles and 347 hr of slagging furnace operation: 145 hr of natural gas firing (including heatup, cooldown, and refractory curing) and 202 hr of coal firing. The longest continuous coal-fired period was 184 hr, completed in April 1999. This summary does not include SFS operation in late March 1999, a planned 200-hr test firing a Powder River Basin subbituminous coal. The next SFS operating period is scheduled for late May 1999. However, specific test objectives and duration have not been determined.

Table 2-7
Summary of Operating Hours for the SFS, CAH Tube Bank,
and RAH Panel Through February 2000

| | Natural Gas Firing, hr | Coal/Lignite Firing, hr | Total Operation, hr |
|-------------------------|------------------------|-------------------------|---------------------|
| Slagging Furnace System | 1737 | 1182 | 2919 |
| CAH Tube Bank | 1422 | 1149 | 2571 |
| RAH Panel | 1238 | 1102 | 2340 |

Task 2.2.5 – Laboratory- and Bench-Scale Activities

In previous, separately funded work performed at the EERC, a temperature window was identified in the thermochemical behavior of the products of coal combustion in which it is believed the products may be much less corrosive toward structural materials. The window ranges from a low temperature of approximately 2000°F (1090°C) to an upper, fuel-dependent temperature of approximately 2300°F (1260°C). The window is believed to exist because above the lower limit, condensed sulfates are not stable in the ash (Hurley and Benson, 1995). Below the upper limit, many coal ashes have very high viscosities so that mass transfer of corrodents to the structural materials are relatively slow and a corrosion-reducing passive layer of corrosion products can exist. At temperatures above the window, the slag is molten and readily dissolves the passive layer, leading to more rapid active corrosion. If such a low corrosion temperature window does exist, then it may be possible to operate the RAH without the protective ceramic tiles between the heat exchanger tubes and the flame. Removal of the tiles would significantly improve heat-transfer rates and simplify the design of the RAH so that time to commercialization of the RAH technology would be significantly reduced.

Therefore, during the last quarter of 1999, coupons of MA-754 alloy were prepared and corroded under controlled laboratory conditions at 2100° F (1150° C). The conditions simulated those experienced by the alloy tubes in the RAH when producing 2000° F (1090° C) pressurized air. This is the highest temperature reached so far during operation of the RAH (see the July–September 1998 quarterly technical progress report). As described in the October to December 1999 quarterly technical progress report, surface recession of the coupons because of corrosion at that temperature was very low. During this quarter, samples from that test were sent to UTRC for further analysis by optical microscopy. UTRC found that numerous pores had formed within the alloy during the corrosion test by a mechanism that is not yet defined. The depth of the visible pore zone was found to be approximately 1/3 of the total cross-sectional area. The presence of these pores will adversely affect physical properties such as ductility and creep resistance. Therefore, although the mechanism of pore formation is not yet understood and the surface recession was low, it was concluded that Alloy MA-754 performed poorly at 2100° F in the presence of coal combustion products.

Although the pore formation indicates that the alloy is not suitable for use without ceramic tile protection at 2100°F (1150°C), it may still be suitable for use at a lower temperature within the sulfate corrosion temperature region of coal combustion products (less than 2000°F, 1090°C). Therefore, during this quarter, five coupons of Alloy MA-754 were cut into 1- × 5/8-in. (2.5- × 1.6-cm) coupons and tested in an enclosed horizontal tube furnace equipped with inlet and outlet ports. The coupons were first subjected to 100 hr of oxidation at 1832°F (1000°C). The coupons were then covered with 0.6 g of Na₂SO₄ to simulate sulfate condensation and topped with a layer of Illinois No. 6 slag to simulate high-temperature coal ash. The samples were then heated in the presence of a simulated combustion gas for 500 hr at 1832°F (1000°C). The gas was composed of 13% CO₂, 4% O₂, 900 ppm SO₂, 9% water, balance N₂ at a flow rate of 0.5 ft³/hr (0.2 L/min). Coupons were removed after 100, 200, 350, and 500 hr of exposure for mass loss calculations. A second coupon exposed for 500 hr was mounted in epoxy with the corrosion and ash layers intact and cross-sectioned for SEM analysis.

Corrosion rates were calculated by mass loss according to ASTM Procedure G1-88. To perform the procedure, the coupons were sonically cleaned in successive chemical baths to remove corrosion

products. The coupons were then weighed after drying, and mass loss from the original oxidized coupon was determined. From the mass loss, a corrosion rate can then be calculated. A plot of the cumulative corrosion is shown in Exhibit 2-28. As the figure indicates, the cumulative corrosion after 500 hr was found to be approximately 0.17 mils (4.4 μm), which suggests a maximum corrosion rate of 3 mils/year (76.4 $\mu\text{m}/\text{year}$). The weighing error for these samples should be no more than approximately 2% relative.

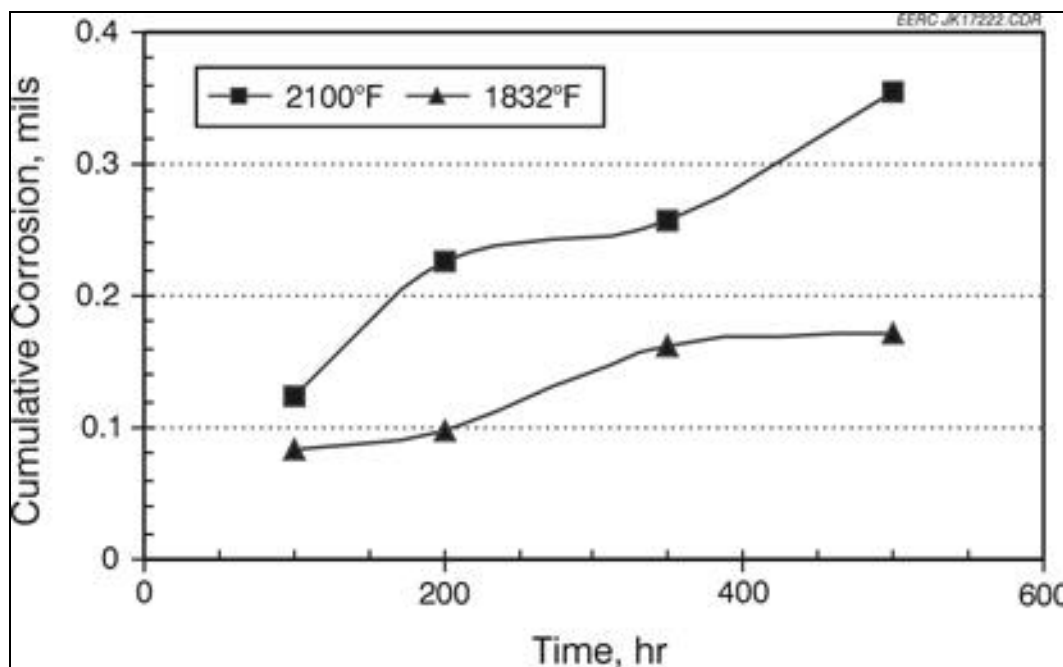


Exhibit 2-28

Cumulative Corrosion of Alloy MA-754 at 2100°F (1150°C) and 1832°F (1000°C)

Exhibit 2-28 also shows a plot of the cumulative corrosion of Alloy MA-754 as determined by the previous test at 2100°F (1150°C). The data indicate that even though the corrosion rate was low at the higher temperature when no condensed sulfate was present, it was still higher by a factor of two than at the lower temperature in the presence of condensed sulfate. This indicated that the low-corrosion window may be more advantageous to alloys which contain more iron in their chemical makeup and are, therefore, more susceptible to attack by condensed sulfates.

The coupon tested for 500 hr that was examined by SEM (scanning electron microscopy) had a discontinuous, irregular chromium oxide layer at the alloy–ash interface that ranged from approximately 0.02 to 0.15 mils (0.5–4 μm). The formation of small pits could be detected, which extended to a depth of 0.3 to 0.4 mils (8–10 μm). An SEM micrograph is shown in Exhibit 2-29. Evidence of chromium oxidation could be detected throughout the entire thickness of the alloy but was more concentrated in a surface zone 1.3 mils (30 μm) deep. The Illinois No. 6 slag had reacted with the sodium sulfate and formed a sintered, porous layer which was lightly attached to the alloy surface. Sulfur was barely detectable in the oxidized zones.

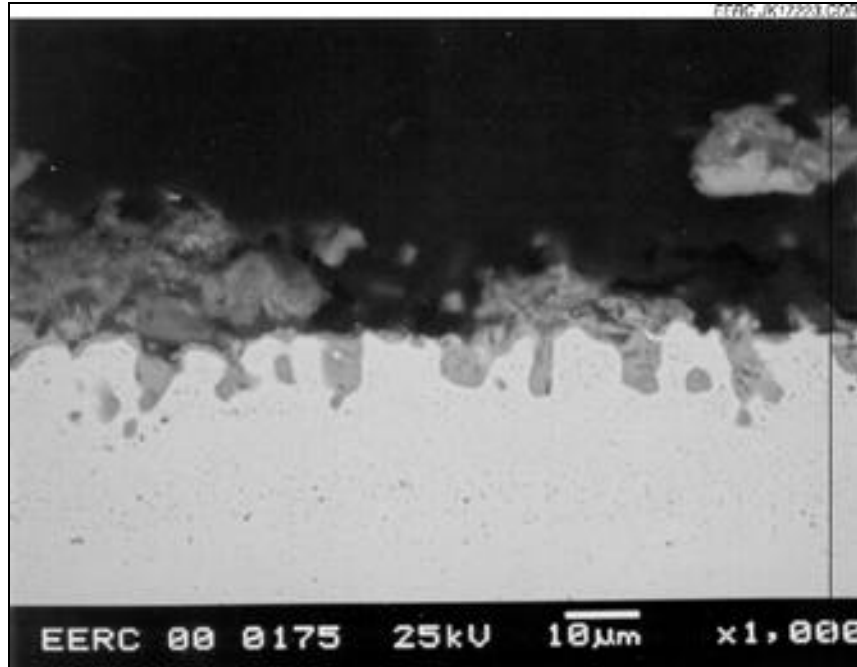


Exhibit 2-29
SEM Micrograph of Alloy MA-754 Showing Oxide Layer

Exhibits 2-30, whose field of view is 1.6 mils (41 μm), and 2-31, with a field of view of 2.2 mils (55 μm), show x-ray maps generated during SEM examination. The chromium oxide layer can be clearly seen. Under these conditions, the chromium reacted with iron in the coal ash to form large iron/chromium oxide crystallites in the ash layer. These crystallites can also be seen in the SEM micrograph shown in Exhibit 2-32. Above the oxide layer, contained in the slag, crystallites can be clearly seen. The formation of these crystallites was not detected in the alloy sample tested at 2100°F (1150°C). Table 2-8 show the spot analysis of the crystallites, surface oxide layer, and zone of oxidation within the alloy.

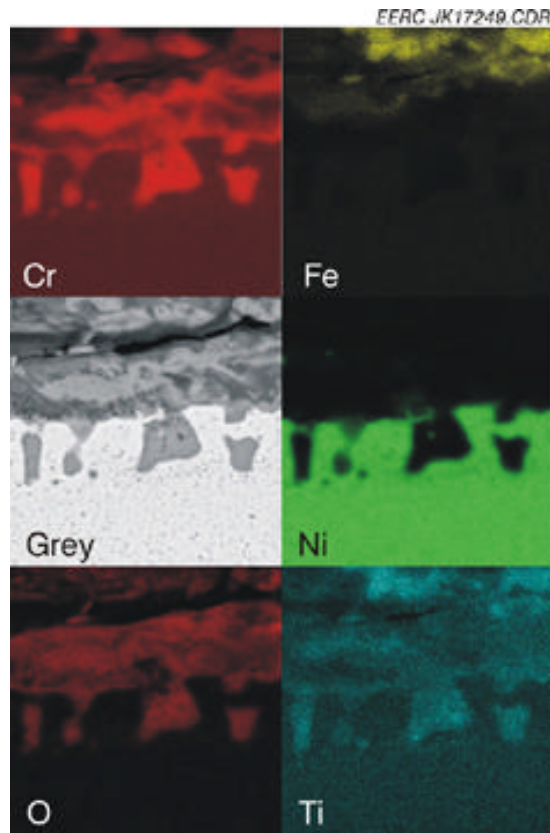


Exhibit 2-30
X-Ray Maps of Alloy MA-754 Showing Oxide Layer

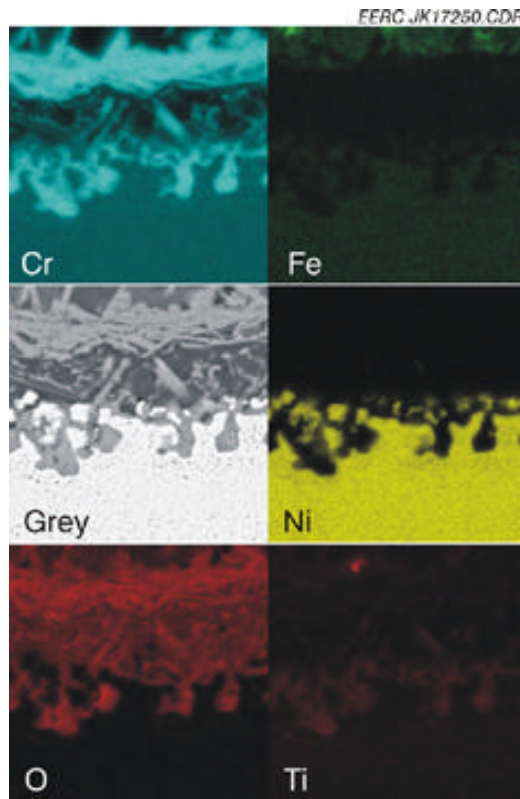


Exhibit 2-31
X-Ray Maps of Alloy MA-754 Showing Crystallites

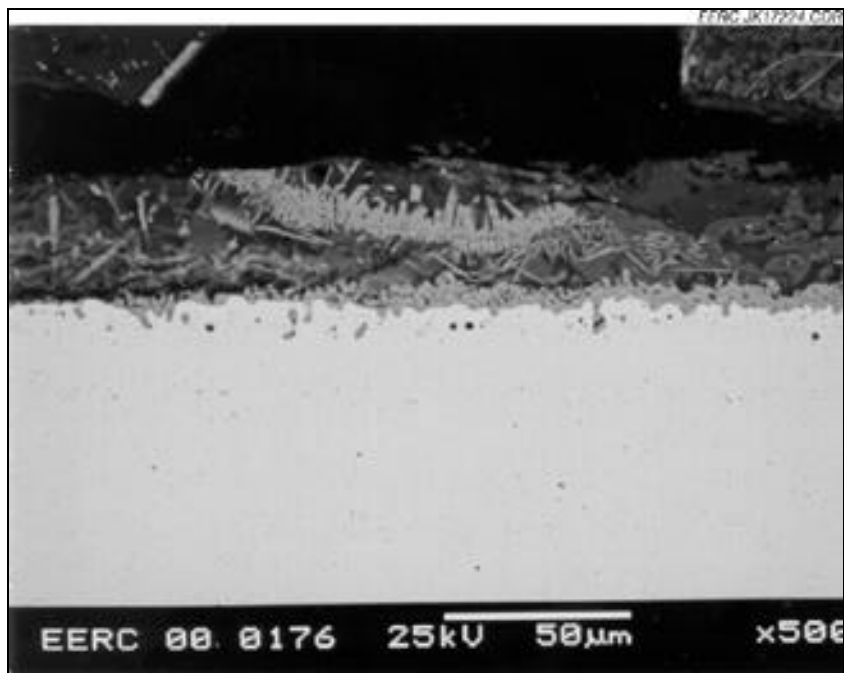


Exhibit 2-32
SEM Micrograph of Alloy Ma-754 Showing Crystallites in the Slag Layer

Table 2-8
Elemental Concentrations of the Oxidation Products, wt%

| Element | Crystallites | | | Surface Oxide Layer | | | Oxidation Zone Within the Alloy | | |
|---------|--------------|------|------|---------------------|------|------|---------------------------------|------|------|
| Cr | 5.5 | 34.5 | 8.4 | 73.4 | 63.2 | 69.5 | 64.5 | 66.0 | 63.8 |
| O | 22.8 | 22.1 | 23.3 | 22.0 | 18.7 | 24.8 | 21.0 | 23.4 | 20.0 |
| Fe | 52.5 | 39.3 | 48.0 | 0.6 | 1.0 | 2.0 | <0.1 | 0.1 | <0.1 |
| Ni | 0.2 | 0.2 | 0.3 | 0.9 | 8.7 | 1.0 | 11.2 | 7.3 | 10.2 |
| Ti | 1.3 | 0.7 | 2.0 | 1.5 | 1.4 | 1.0 | 1.7 | 1.7 | 2.8 |
| Al | 4.4 | 0.7 | 4.0 | 0.2 | 1.2 | 0.3 | 0.7 | 0.4 | 2.3 |
| Ca | 0.9 | 0.2 | 0.7 | 0.2 | 0.5 | 0.3 | 0.2 | 0.2 | 0.1 |
| Nb | ND | 0.2 | ND | ND | <0.1 | <0.1 | ND | 0.2 | ND |
| Si | 8.6 | 0.9 | 6.9 | 0.8 | 4.5 | 0.7 | <0.1 | ND | <0.1 |
| Na | 2.6 | 0.4 | 4.3 | ND | <0.1 | <0.1 | ND | ND | ND |
| S | 0.2 | 0.1 | <0.1 | ND | 0.1 | <0.1 | ND | ND | ND |

Task 6.4 HIPPS Repowering

6.4.1 Performance

The attractiveness of HIPPS in repowering applications has been described in previous reports. This potential of HIPPS repowering has been given a boost because of the added benefits that could accrue were Vision 21 (V21) technologies included as part of the repowering. One such technology is the solid oxide fuel cell, a high temperature fuel cell that operates at approximately 1800 F. A schematic of a potential HIPPS/solid oxide fuel cell hybrid used to repower the nominal 121 MW, 34% efficient site in New York State is shown in Fig. 6.4.1. The SOFC operating temperature level is easily reached at the radiator outlet in the HITAF. The compressor discharge air is heated in the HITAF and then sent to the cathode of the SOFC. Natural gas is completely desulfurized, mixed with steam and sent to the anode of the SOFC. A slipstream can be sent to the GT, if desired. However, the anode exhaust from the fuel cell contains H_2 , CO , and some CH_4 , which is burned in the duct burner of the GT.

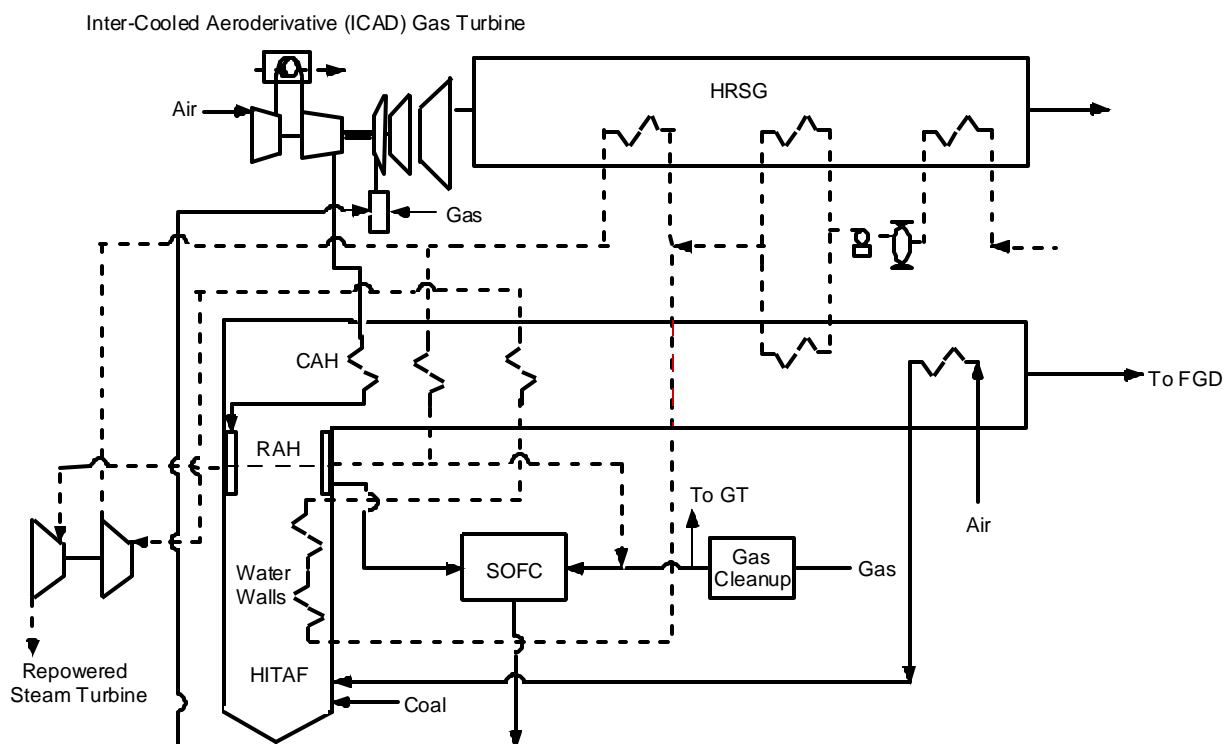


Exhibit 6.4.1
Schematic of HIPPS/SOFC Repowering

Several variations of this plant were investigated, based on the fraction of system heat supplied by coal: 60% coal, 50% coal, and 40% coal. The results are given in Table 6.4.1. At 60% coal, the efficiency is slightly over 50% (HHV), at 50% coal the efficiency is over 55%, and at 40% coal, the efficiency is over 61%. An additional variation was also investigated in which the turbine inlet temperature was determined by the combustion of the SOFC exhaust with no additional gas fuel. Here, the gas fraction was nearly 38% and the overall efficiency was 52.4% (HHV).

Table 6.4.1
HIPPS/SOFC Performance

| Engine Type | HITAF | HITAF | HITAF | HITAF |
|-----------------------------------|---------------|---------------|---------------|---------------|
| Type of fuel | FT4000 | FT4000 | FT4000 | FT4000 |
| | Coal & Gas | Coal & Gas | Coal & Gas | Coal & Gas |
| %Gas | 61.0 | 50.0 | 40.0 | 37.9 |
| Inlet Air Flow/engine, lbs/sec | 610.3 | 610.3 | 610.3 | 610.3 |
| OPR, PR(HPC*LPC) | 60.3 | 60.3 | 60.3 | 60.3 |
| GT Turbine Inlet Temp, F | 2716 | 2716 | 2716 | 2200 |
| System Performance | | | | |
| Total net power, MW (@gen) | 647.8 | 431.4 | 309.9 | 322.9 |
| Gross Gas Turbine power, M | 176.4 | 154.1 | 141.7 | 97.5 |
| Gross Steam Turbine power, MW | 128.3 | 113.1 | 104.9 | 99.4 |
| Gross Fuel Cell power, MW | 351.2 | 171.4 | 70 | 132.1 |
| Cycle Efficiency, gross (HHV c&g) | 61.2 | 55.6 | 50.3 | 52.4 |
| Gas Turbine Performance | | | | |
| GT HPT temp, F | 2716 | 2716 | 2716 | 2200 |
| GT LPT temp, F | 1964 | 1895 | 1852 | 1422 |
| GT exhaust temp, F | 775 | 726 | 696 | 505 |
| GT Stack temp, F | 180 | 180 | 180 | 180 |
| Fuel flow/engine, lbs/sec | 26.00 | 15.65 | 10.00 | 0 |
| HITAF Combustor | | | | |
| Coal flow rate, lbs/sec | 31.4 | 29.6 | 28.4 | 29.3 |
| Radiant sect., GT Outlet temp, F | 1634 | 1754 | 1803 | 1774 |
| Convective HX outlet temp, F | 1300 | 1300 | 1300 | 1300 |
| HITAF HRSG stack temp, F | 596 | 551 | 517 | 429 |
| Steam System | | | | |
| HP Throttle flow, lbs/sec | 198.1 | 174.7 | 162.2 | 153.8 |
| HP pressure/temp, psia/F | 1477/9 | 1477/9 | 1477/9 | 1477/9 |
| | 56 | 56 | 56 | 56 |
| LP Steam flow, lbs/sec | 198.1 | 174.7 | 162.2 | 153.8 |
| LP pressure/temp, psia/F | 454/10 | 454/10 | 454/10 | 455/10 |
| | 08 | 08 | 08 | 08 |

6.4.2 Economic Comparison

While the addition of the SOFC improves the performance of the repowered plant, it would be instructive to identify the cost benefits of such additions. The lack of actual cost information on the advanced power systems necessitates a relatively simplistic approach to be taken for the economic analysis. The original baseline steam plant was assumed to have an overnight cost of \$1200/kW, fuel cost of \$1.00/million Btu, and non-fuel O&M costs of 4 mills/kWh. The cost of power was calculated for a load factor of 65% and normalized to a value of one. The cost of electricity (COE) for the HIPPS and HIPPS/SOFC repowered systems were then compared on this normalized basis.

Depending upon what upgrading was required by the existing infrastructure, the cost of repowering with HIPPS has been estimated to be between \$600 and \$800/kW of incremental power, as documented in earlier reports. The \$800/kW value was used for the HIPPS repowering, as the switchyard and ash handling required upgrading. For the SOFC/HIPPS, \$810/kW was used for the HIPPS portion, as the steam turbine also required upgrading. The non-fuel O&M costs were assumed to be 7 mills/kWh including an allowance for refractory replacement in the HITAF. Cost estimates for the SOFC range from \$100's/kW to over \$3000/kW. Based on updating a SOFC repowering study done by Bechtel in 1992, a value of \$1000/kW was assumed. The non-fuel O&M costs for the SOFC were assumed to be 9 mills/kWh. This includes an allowance for materials to replace the fuel cell modules after 40,000 hr.

The remaining major variable in the COE calculation is the cost of fuel. At this time, natural gas supplies are plentiful at a cost somewhat more than twice that of coal. It is predicted that gas supplies will remain plentiful, but infrastructure requirements may limit the availability and competition for end use could increase the costs. Projections of the cost of gas for utility use by the Energy Information Agency indicate an increase by 40 % over the next twenty years (Fig. 6.4.2). The same source predicts coal costs will remain nearly constant and could actually drop as fuel competition increases. The analysis shown in Fig. 6.4.3 uses gas-to-coal cost ratios projected for the year 2000 (2.5), for 2010 (3.0), and 2020 (3.5) to compare COE for the repowering cases.

For repowering, the use of gas in combination with the coal makes a good deal of economic sense. The GT or GT/SOFC portion of the plant can be operated independently; creating a revenue stream during planned, or forced, outages of the coal portion. This dual fuel approach offers considerable operating flexibility.

In Fig. 6.4.3, it can be seen that the COE for the HIPPS repowering is lower than those for the HIPPS/SOFC repowering scenarios for all fuel cost ratios. The higher capital costs of the HIPPS/SOFC and the higher cost of gas relative to coal are not offset by the efficiency gains. An all-gas-repowering scenario (SOFC/GT, but no HIPPS) had a lower capital cost and an efficiency of 61.4% (HHV). Its COE was still higher than those schemes using coal, even at the lowest gas/coal cost ratio.

The removal of greenhouse gases such as CO₂ may change the economics. At this time the costs for CO₂ reduction are not well defined. An assessment of the impact of the removal of CO₂ on COE can be seen by imposing a "carbon tax"; e.g., a tax of 350 NOK (~\$55) per metric ton of CO₂ has been set by the government of Norway on emissions from combustion

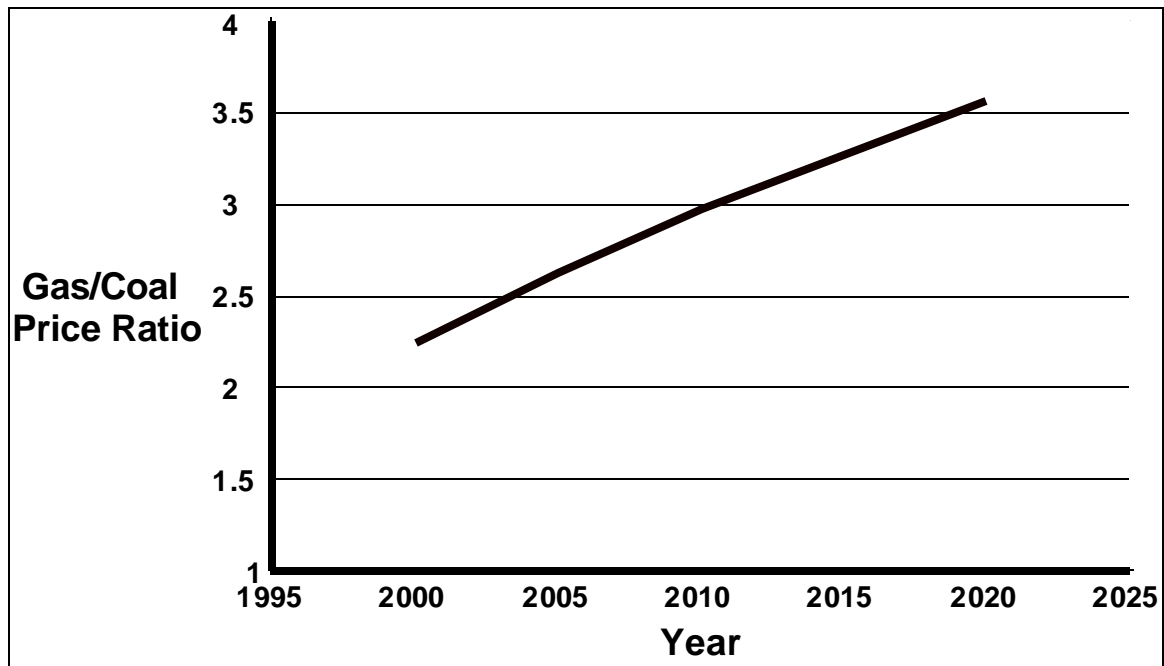


Exhibit 6.4.2
Projected Fuel Cost Ratio

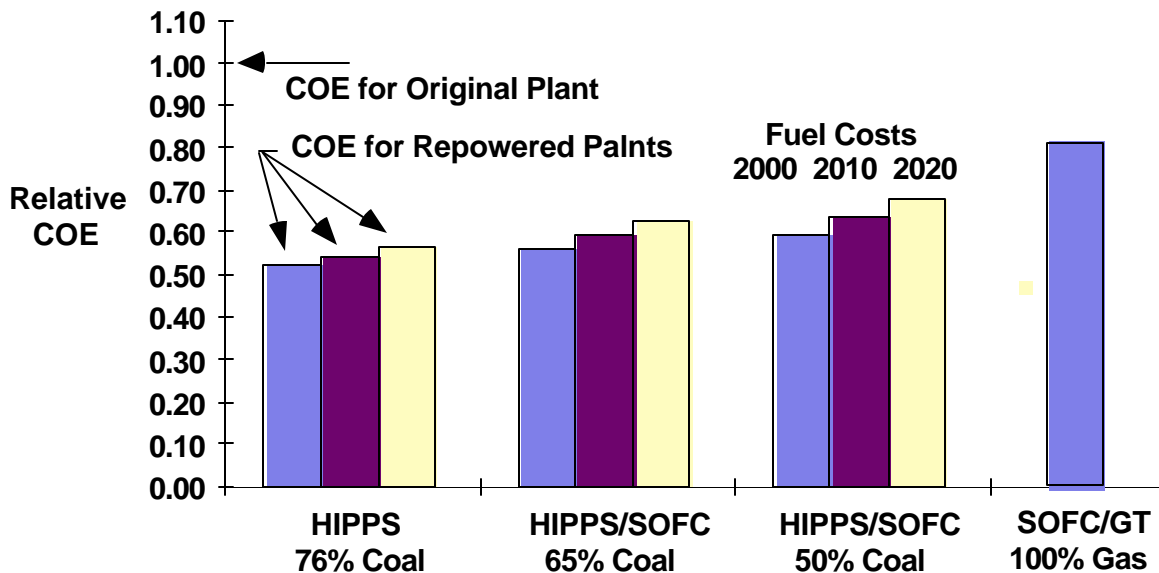


Exhibit 6.4.3
Relative Cost of Electricity

The effect of imposing such a tax on the foregoing repowering scenarios is shown in Fig. 6.4.4. A coal-fired plant having an efficiency of 34% (the baseline plant to be repowered) would have CO₂ emissions of about 1 kg/kWh. At a tax of \$55/tonne, the additional cost would be approximately \$0.055/kWh, a value that would more than double the cost of electricity. Since the object is to compare the various HIPPS configurations, once again the cost of electricity has been normalized against the original plant cost, this time with three values for CO₂ removal, \$55, \$27.50 and \$13.75/tonne CO₂.

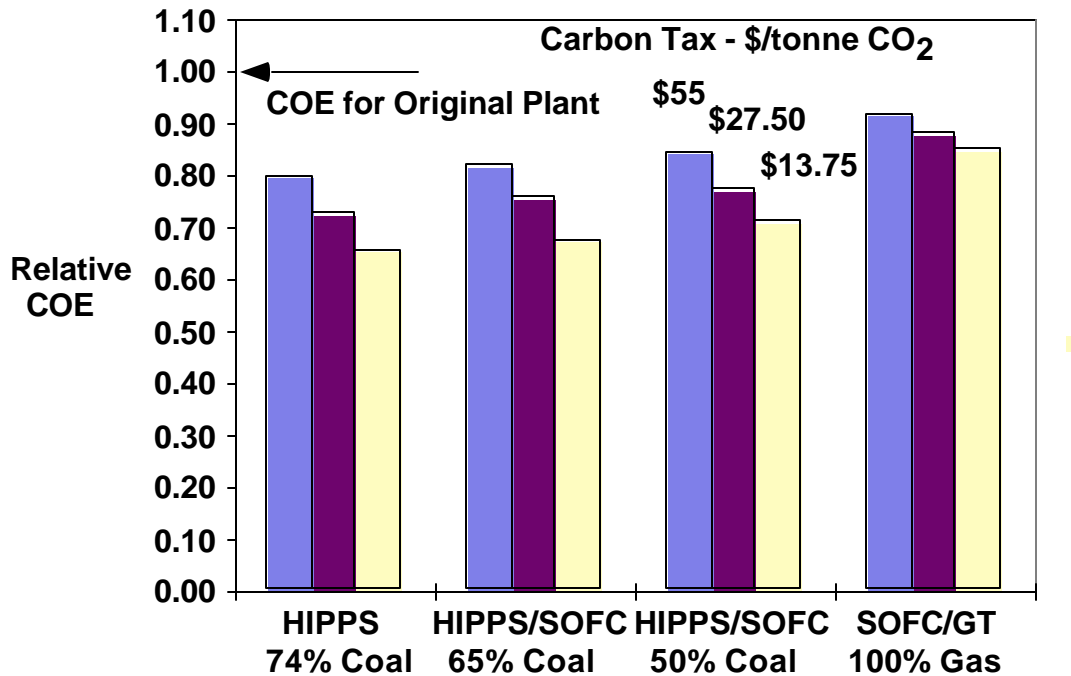


Exhibit 6.4.4
Relative COE with CO₂ Removal

As before, the added efficiency of the configurations with the SOFC do not overcome their higher capital and fuel costs, although the percentage differences in the relative costs have been reduced because of the lower costs of CO₂ removal from the more efficient configurations.

6.4.3 Repowering of AFB Plant

Previous analyses have been based on repowering of a steam plant located in upper New York State. Recently, Bechtel has obtained the specifications of an Atmospheric Fluid Bed (AFB) plant located on the TVA system. This plant, shown in Fig. 6.4.5, is a candidate for replacing the AFB. The plant has a nominal output of 160 MW with a net output of 151.6 MW at a heat rate of 9244 Btu/kWh (36.9% efficiency HHV). The steam conditions are 1815 psi/1000 F /1000 F.

A preliminary analysis of a HIPPS repowering of this system results in efficiencies over 45% with 77% coal heat input. Details of this system and of variations using the hybrid HIPPS/SOFC will be reported in the next reporting period.

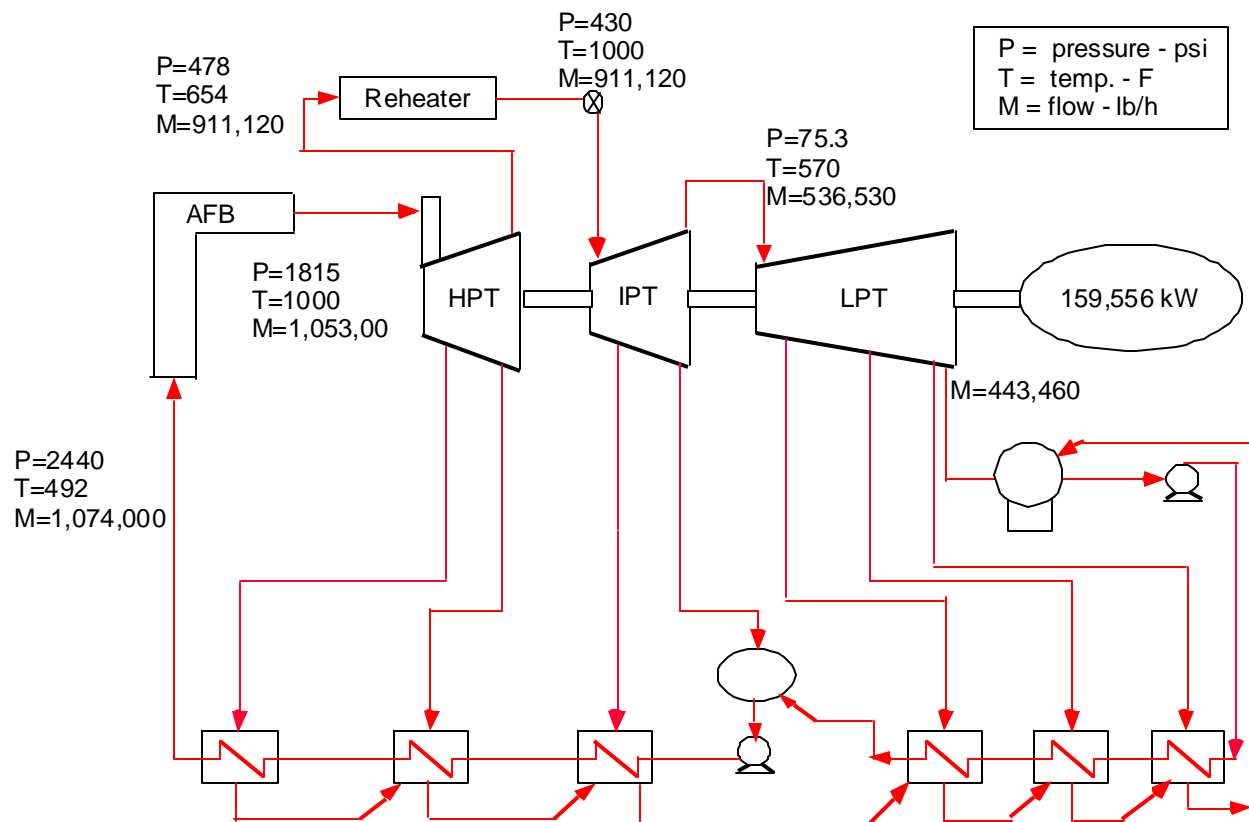


Exhibit 6.4.5
Schematic of Nominal 160 MW TVA AFB

Reference

Hurley, J.P.; Benson, S.A. Ash Deposition at Low Temperatures in Boilers Burning High-Calcium Coals: 1. Problem Definition. *Energy Fuels* 1995, 9, 775–781.